MODELING THE GROUNDWATER BASIN IN THE NORTHERN CITIES MANAGEMENT AREA

A Thesis

presented to

the Faculty of California Polytechnic State University,

San Luis Obispo

In Partial Fulfillment

of the Requirements for the Degree

Master of Science in Civil and Environmental Engineering

by

Allyson Nichole Swain

June 2021

COMMITTEE MEMBERSHIP

TITLE:	Modeling the Groundwater Basin in the Northern Cities Management Area
AUTHOR:	Allyson Swain
DATE SUBMITTED:	June 2021
COMMITTEE CHAIR:	Misgana Muleta, Ph.D., P.E., D.WRE Professor of Civil and Environmental Engineering
COMMITTEE MEMBER:	Rebekah Oulton, Ph.D., P.E. Associate Professor of Civil and Environmental Engineering
COMMITTEE MEMBER:	Daniel Heimel, P.E. Water Systems Consulting

ABSTRACT

Modeling the Groundwater Basin in the Northern Cities Management Area

Allyson Nichole Swain

A model was developed to simulate the groundwater of 8,300 acres of the Northern Cities Management Area (NCMA), which encompasses the northern portion of the Arroyo Grande Watershed and a small subset of the Santa Maria Valley Groundwater Basin. This watershed and groundwater basin is located on the coast and contains Oceano and the Cities of Arroyo Grande, Grover Beach, Pismo Beach. Groundwater in the NCMA is used heavily for agricultural irrigation in the southern portion and municipal applications in the northern portion. Up to 18 of these municipal wells and over 50 irrigation wells are drawing groundwater at any time. Due to the critical nature of both uses, and location on the coastline, both supply and quality is a significant concern. The objective of this research was to improve an existing groundwater model with a longer model duration, a more detailed and discretized recharge estimation, and incorporation of addition municipal well data. Some data was preprocessed in ArcMap. Groundwater modeling was accomplished with Aquaveo GMS using MODFLOW-NWT upstream weighting package (UPW). Elevation, hydrologic soil conditions, stream gauge heights and flows, recharge rates, fault locations, well locations and pumping rates, and transient head boundaries were created via coverages in GMS and mapped to MODFLOW. The model was calibrated using Parameter Estimation (PEST) with Singular Value Decomposition-Assist (SVD-Assist) to observation data in six select monitoring wells and fifteen Sentry wells. The model showed outflow from the domain to the ocean with groundwater flows shifting to parallel the coast following dry periods and significant simulated drawdown from one particular municipal well. These trends can provide water purveyors in the area with additional information on groundwater trends and effects of pumping rates on formation drawdown.

ACKNOWLEDGMENTS

I would like to thank my advisor Dr. Muleta for his endless patience and support both with this thesis and throughout my time at Cal Poly. I would also like to thank my committee members, Dr. Oulton and Daniel Heimel. Dr. Oulton supported me immensely through Senior Project and pushed me to be the engineer I am today. Dan Heimel took time out of his busy schedule to ensure I had the data and connections I needed.

Thank you to the other CE and ENVE professors and fellow students at Cal Poly that made my college experience so wonderful and successful.

And last, thank you to my family and friends for supporting me and encouraging through the whole process.

Table of Contents

Page

Page

LIST OF FIGURES

LIST OF TABLES

Tables Page

1. Introduction

Groundwater is the part of the natural water cycle held underground in the voids and crevices of soil and rock. Groundwater can surface naturally via a spring or as recharge to waterways. However, we most commonly see groundwater extraction using a well. Use of wells for groundwater extraction dates back over 7,000 years to the Early Neolithic period in the Czech Republic and in China.

In the United States, over 50% of the population relies on groundwater for drinking water. However, the largest use of groundwater by volume is for the irrigation of crops (Groundwater Foundation, n.d.). This reliance can prove detrimental when groundwater supply faulters. In recent history, California and other western parts of the country have experienced multiple droughts, most notably from 1928-1934, 1987-1992, and 2012-2016 (USGS, n.d.). During times of drought, reliance upon groundwater often increases, exacerbating the problem (USGS, n.d.).

Besides decreased groundwater supply resulting in water level drops and well drying, land subsidence and saltwater intrusion can also occur. Land subsidence occurs when underlying aquifers contract and their structural support is lost for ground above. Over pumping, starting in the 1920s, has caused permanent subsidence up to 28 feet in sections of the San Joaquin Valley (NASA Earth Observatory, 2016). From 1960 to 2016, the State of California had spent over $100 million on repairs related to subsidence (NASA Earth Observatory, 2016). In coastal areas or areas near briny water, over pumping can decrease the water levels to the point where saltwater infiltrates the aquifer, potentially ruining the quality of the supply for all users.

In order to help manage and prevent further overdraft, California governor Jerry Brown signed a three bill legislative package that became known as the Sustainable Groundwater Management Act (SGMA). In May of 2016, the California State Water Board implemented SGMA which requires local agencies to form groundwater sustainability agencies and to adopt groundwater sustainability plans. Groundwater sustainability agencies must achieve sustainable groundwater management within 20 years with an absolute deadline of 2040 and 2042 for critically over drafted and high to medium priority basins respectively (State Water Resources Control Board, 2020).

One of the best ways for agencies and regions to manage their groundwater is by using models calibrated with historical data to predict future groundwater levels and supply. Models can also be used to test the effects of different artificial recharge applications or demands on the water supply and distribution. However, modeling has been continually advancing, both in the software capabilities and the data available for modeling.

The objective of this study is to re-develop and expand a groundwater model for the Northern Cities Management Area (NCMA) in the Arroyo Grande Watershed from Brian Wallace's 2016 thesis report with more detailed data over a longer timeframe and compare the results to previous studies for cross validation.

1.1. Background

The area of interest for this study is the Northern Cities Management Area (NCMA) which lies on the central coast of California, east of Highway 101. The NCMA is a sub-area of the Arroyo Grande Watershed and the northern most portion of the Santa Maria River Valley Groundwater Basin. The management area is a more than 30 year old joint effort by the Northern Cities: City of Arroyo Grande, City of Pismo Beach, City of Grover Beach, and the Oceano Community Service District. A 2005 Stipulation for the Santa Maria Groundwater Basin Adjudication (2005 Stipulation) and a 2008 Judgement after Trial (2008 Judgement), by the Superior Court of California, County of Santa Clara, requires the Northern Cities to conduct groundwater monitoring including:

- Land and water use in the basin,
- Sources of supply to meet those uses,
- Groundwater level and quality conditions

This area has a variety of users and terrain including domestic households, industrial sectors, agriculture, and natural dune areas.

Figure 1. Study Area Location with Boundary in Yellow and Relevant Cities in White

1.1.1. Arroyo Grande Watershed

The Arroyo Grande Watershed is 95,998 acres with a maximum elevation of 3,100 feet above mean sea level (amsl) and terminating at the Pacific Ocean. Much of the watershed is used for agriculture consisting of primarily vineyards, ranches, and row crops. The watershed also contains an urban core in the lower elevations, a regional airport near Oceano, and Lake Lopez Reservoir. Groundwater basins in the Arroyo Grande Watershed consist of the Santa Maria River Valley Basin, the Arroyo Grande Creek sub-basin, and the Edna Valley Basin (SLO County, n.d.).

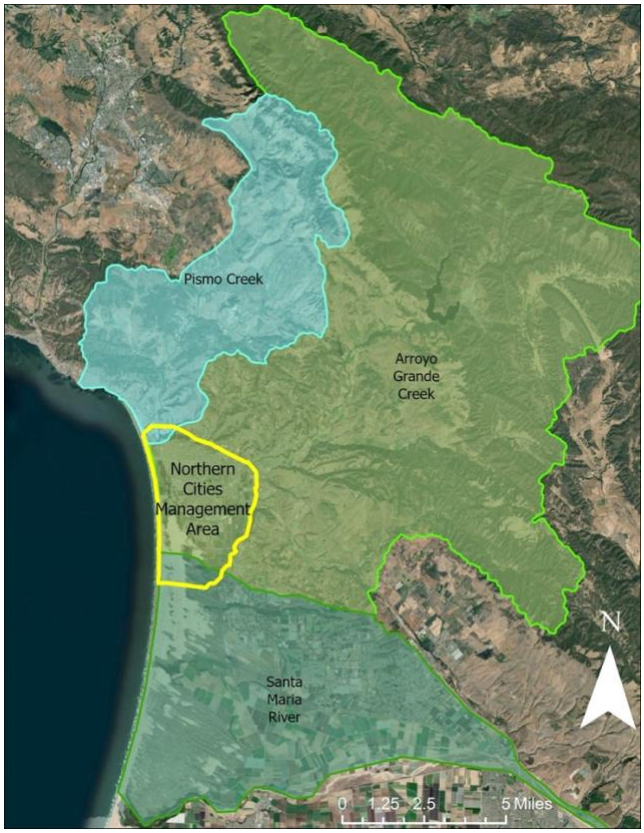

Figure 2. Northern Cities Management Area within Surrounding Watersheds

1.1.2. Santa Maria River Valley Groundwater Basin

The Santa Maria River Valley Groundwater Basin (SMGB) is a DWR high priority basin split between northern Santa Barbara County and southern San Luis Obispo County. It covers approximately 184,000 acres with the majority of groundwater stored unconfined in alluvium, dune sands, and the Orcutt, Paso Robles, Pismo, and Careaga formations. Confined groundwater does exist in the coast area of the basin (SLO County, n.d.).

Rights to pump from the SMGB has been in litigation since the 1990s (GSI Water Solutions, Inc, 2019). SGMA does not apply to the NCMA area as long as the requirements of the 2005 Stipulation and 2008 Judgement are met. Fringe areas around the NCMA do fall into the jurisdiction of SGMA and are managed appropriately.

Figure 3. Northern Cities Management Area within Santa Maria River Valley Groundwater Basin

1.1.3. Urban Water Use

Approximately 17.6% of the watershed is urbanized, with the majority of this as residential area. Each of the four cities have their own public utility district with a combined total of 19 actively pumping wells. Urban demand, consisting of both ground and surface water, has fallen 34% from 8,615 AF in 2005 to 5,660 AF in 2019. These decreases are attributed to the slowing economic growth and conservation policies put in place by the NCMA. In 2019, groundwater accounted for only 12% of the potable urban supply, however this was only 17% of the groundwater allotment for the year (GSI Water Solutions, Inc, 2019).

1.1.4. Agricultural Water Use

Agriculture encompasses much of the southern part of the NCMA. The 2019 Annual Crop Report by the San Luis Obispo County Department of Agriculture estimates 1,463 acres of irrigated crops within the NCMA. The majority of irrigated lands in the

NCMA is rotational crops where two to three different products are grown per year. These could be any combination of broccoli, cabbage, cauliflower, celery, kale, lettuce head, lettuce leaf, and spinach (SLO County Department of Agriculture, 2020).

1.1.5. Environmental Water Use

The NCMA has two main creeks, the Arroyo Grande Creek and Los Berros Creek, both of which are highly channelized in the study area. Los Berros Creek joins Arroyo Grande Creek approximately 2,000 feet upstream of the Hwy 1 bridge, however Los Berros frequently runs dry. Both Arroyo Grande Creek and Los Berros Creek are designated Steelhead Trout stream and designated critical habitat for:

- South-Central California Coast Steelhead Trout,
- California Condor,
- California red-legged frog,
- La Graciosa thistle,
- Western snowy plover

Pismo Creek acts as the northern boundary of the NCMA and terminates directly into the ocean via a small lagoon. Water level in this waterway is not only dictated by upstream supply but also shifting sand bars that can limit discharge to the ocean.

1.2. Previous Work

Many studies have been done in the Santa Maria Valley Groundwater Basin (SMGB), with only a few specifically focusing on the NCMA area.

The most recent California Department of Water Resources (DWR) report from 2002 studied a portion of the SMGB with a southern boundary of the SLO and Santa Barbara County line, encompassing a total of 117,940 acres. Water years 1975 through

2000 were considered and the study was split into three sub-areas: the Tri-Cities Mesa, Arroyo Grande Plain, and Santa Maria River Plain. The NCMA most closely matches the Tri-Cities Mesa area. The DWR detailed how the basin included multiple significant geological deposits such as the Pismo, Careaga, Paso Robles, and Orcutt Formations, as well as alluvium and dune sand. DWR lists both the alluvium and the Paso Robles Formation as the most productive zones consisting of unconfined conditions with localized semi-confined to confined pockets and perched zones. Trends of historical groundwater contours revealed that overall groundwater moved seaward in a "westerly to west-northwesterly direction" but more "southwesterly in the Arroyo Grande Valley" (Department of Water Resources, 2002).

Fugro Consultants, in collaboration with GEI Consultants, prepared the Santa Maria Groundwater Basin Characterization and Planning Activities Study in December of 2015 for the San Luis Obispo County Flood Control and Water Conservation District. As the title describes, this study focused on the SMGB as a whole but had exhaustive summaries of past reports, geological studies, pumping and drawdown tests, evaluation of stream infiltration, evaluation of offshore aquifer and seawater intrusion. Zone 1, area south of the Wilmar avenue fault and north of the Santa Maria River fault is representative of the NCMA in this study. Fugro found that pumping tests, using the Driscoll 1986 method for specific capacity and relative thickness based on screen lengths, showed an average horizontal hydraulic conductivity of 115-270 feet/day and 12-13 feet/day for the Paso Robles and Careaga Formations, respectively (Fugro Consultants, Inc., 2015).

One of the most recent and extensive documents is Central Coast Blue's 2018 Phase 1B Hydrogeologic Evaluation, which is a collection of various Technical Memorandums. Central Coast Blue is a collaboration between five agencies: the City of Arroyo Grande, the City of Grover Beach, the City of Pismo Beach, Oceano Community Services District, and South San Luis Obispo County Sanitation District. GEOSCIENCE prepared the Model Boundaries Technical Memorandum (2018) describing the mountain front recharge, general head, and bedrock boundaries, including the general head boundary for the ocean (GEOSCIENCE, 2018).

GEOSCIENCE also prepared the Agricultural Estimate Technical Memorandum for a surface water balance and to estimate agricultural irrigation demand. They estimated a 12% decrease in ET data from the inland CIMIS station and created evapotranspiration (ET) type curves based on crop for various annual precipitations. From there they were able to estimate annual agricultural irrigation production and compare this to the NCMA results (GEOSCIENCE, 2018).

The Phase 1B Technical Memorandum 1: Conceptual Model, prepared by Water Systems Consulting and GEOSCIENCE, modeled the NCMA for the purpose of analyzing injection and extraction options of advanced treated water from the City of Pismo Beach and South San Luis Obispo County Sanitation District (SSLOCSD) wastewater treatment plants. However, this model was expanded to include the Nipomo Mesa Management Area (NMMA) and the Santa Maria Valley Management Area (SMVMA) to decrease the number of boundary errors. Model layers and topography was created using a 3-D lithological model with more than 400 lithological logs resulting in

10 model layers. Cells were 100 x 100 feet and the model was run with SEAWAT (a USGS model) from 1977 to 2016 (GEOSCIENCE & Water Systems Consulting, 2018).

However, the scope of this study mainly stems from previous work completed in 2016 by Brian Wallace for the partial fulfillment of the requirements for the degree of Master of Science in Civil/Environmental Engineering from Cal Poly. The study focused on the same study area with a model period of January 2008 to December 2015. After calibration of the model, Brian compared his aquifer storage and overall water balance to the 2007 Todd Engineer's Water Balance for the Northern Cities Area. Calibration produced mixed results where one set of optimal parameters provided a good fit to hydrographs (simulated vs observed head) whereas another set provided a better fit to the 2007 Todd Engineering Water Balance Study for the Northern Cities Area flow budget. A solution that optimized both targets was unable to be accomplished with this model (Wallace, 2016) .

1.3. Purpose and Objectives

The purpose of this study is to expand upon the previous NCMA model developed by Brian Wallace in 2016. His study's objective was to "develop a numerical groundwater model for the NCMA aquifer system to enhance the understanding of groundwater flow". This project is intended to expand the model time frame from the previous period of 2008 to 2015 to 2008 to 2019. Additional data sources such as the City of Pismo Beach wells and pumping data will be included to better describe the northern model region. Irrigation demand will also be further developed using more detailed crop coefficients and water balance methods. Transient boundaries will be developed to replace constant head boundaries, better simulating the area's interaction with the larger

groundwater basin. Hydraulic characteristics from this improved model will be compared to previous models and studies in the area for validation. The model will also be analyzed for general groundwater elevation trends.

Because of this area's proximity to the ocean and large agricultural presence, saltwater intrusion and groundwater availability are significant concerns that a model can help manage. Both of these issues may be further exacerbated with climate change and lower surface water availability, causing a greater reliance on groundwater. Further work in this model could yield a simulation that could potentially be used by water purveyors in determining safe yields and optimal areas for recharge.

2. Data

The data described in this chapter was used to build the conceptual GMS model. Some values described in this section are initial values that were later calibrated to simulate observed hydraulic head values.

2.1. Boundaries

The Pacific Ocean defines the western boundary, although the SGMA is hydraulically continuous offshore up to 12 miles (Department of Water Resouces, 1979). The ocean was modeled as a general head boundary set to mean sea level (0 feet amsl) with an initial conductance of 0.02 $ft^2/day/ft$ for the top layer only (shown in red in Figure 4). This initial value was based off an example from the USGS also using a GHB for an ocean-aquifer contact (USGS, 2013).

Conductance for the general head boundary is based off the transmissivity (hydraulic conductivity times the aquifer thickness) divided by the distance from the ocean to the boundary (assumed as the width of one cell, 125 ft) per unit length of the boundary. However, after initial calibration, hydraulic conductivity was much different than expected and the initial conductance was changed to 12.4 $ft^2/day/ft$ based off an average hydraulic conductivity of 47 ft/day and thickness of 32 ft. A limit of 102 $ft^2/day/ft^2$ was assigned for this boundary due to a maximum possible hydraulic conductivity of 400 ft/day, as described in section 2.3.

The eastern boundary is politically defined by the management area but has a geological change from alluvium to an outcropping of Paso Robles Formation or older dune sands. Because of the outcropping, this boundary is a no-flow boundary. However, there is connection in this area with the rest of the Santa Maria River Valley groundwater

basin and potential mountain front recharge. To model these interactions, the eastern boundary south of the Arroyo Grande Creek was changed to a transient head boundary (time variant specified head boundary) with values interpolated from the NCMA annual report groundwater contours (shown in purple in Figure 4). The stream package also regulates head in the few cells the stream spans on the eastern boundary.

Highway 101 acts as the unofficial northern boundary but is more specifically the surfacing of Squire Sandstone, the oldest formation in this study area which was modeled as bedrock. This is also modeled as a no-flow boundary.

The southern boundary has no clear geological significance and is assumed as a purely political choice. This boundary was modeled with a transient head boundary created from groundwater elevation contour values from past NCMA reports. More information about the creation of the transient boundary and observation data is given in section 2.9.

2.2. Layers and Elevation

The model consists of three layers based on the geologic conditions of the area.

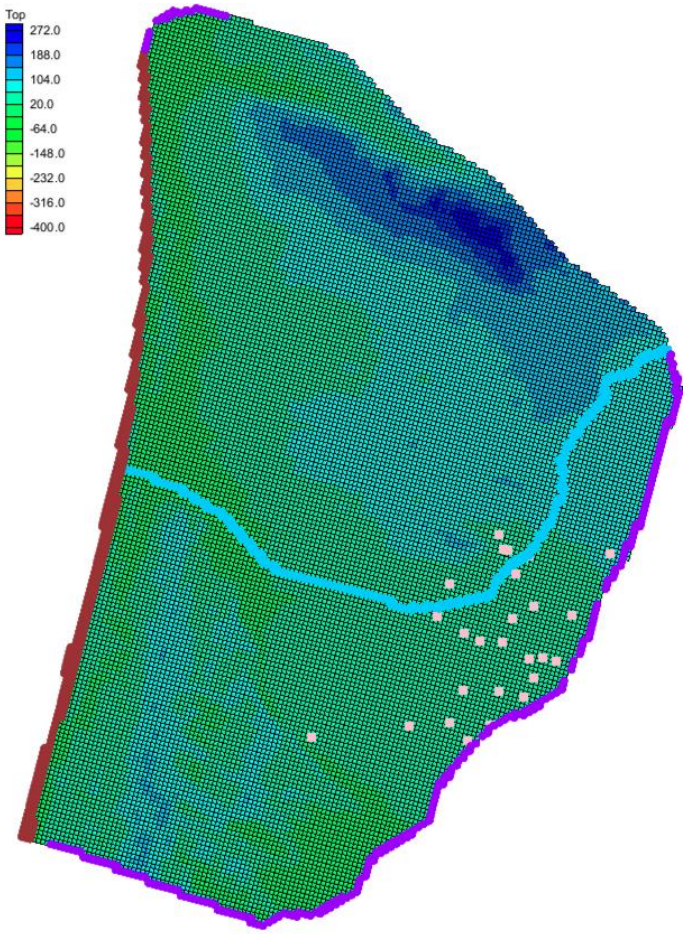

Figure 4. Topy Layer of the Model with Elevation Shading, General Head Boundary in Red, Transient Boundary in Purple, Stream in Aqua, Wells in Pink

2.2.1. Top Layer

The top layer (Layer 1) is a mix of alluvium and dune sands. Dune sands dominate the upper layer in the Tri-Cities Mesa and western portion of the NCMA with a thickness range of 20 to 60 feet and have been shown to have perching layers of clay. The dune sand varies in age depending on location and depth from 40,000 to 120,000 years old but is generally categorized as fine to coarse grain sand with some silt and clay

(Fugro Consultants, Inc., 2015). Holocene Alluvium is more prevalent on the eastern side of the NCMA along the Arroyo Grande Creek. It is 130 feet deep at the juncture of Los Berros Creek and Arroyo Grande Creek (Department of Water Resources, 2002), and is the youngest of all soils and formations and comprised of sand, gravel, silt, and clay, with cobbles and boulders (Fugro Consultants, Inc., 2015). The ground surface, top of layer 1, came from a 1/3 arc second digital elevation model (DEM) from the USGS data download portal. This layer was modeled as convertible which allows confinement to be determined on a cell-by-cell basis, with a default of unconfined. Even though this layer has historically been categorized as completely unconfined, MODFLOW-NWT only allows layers to be assigned as convertible or confined.

2.2.2. Middle Layer

The middle layer (Layer 2) is the Paso Robles Formation and varies in the SMGB from 200 to 700 feet thick (Department of Water Resources, 2002). It is comprised of many lenses of fine to coarse sand and gravel, clayey to silty sand and gravel, and medium silty sand. In many areas the clay is around 50 to 100 feet thick with much of the coastline having a confining layer of clay defining the contact between the Paso Robles and Careaga Formations. However, there are also some areas where the Paso Robles Formation directly overlays the Careaga Formation with some areas being difficult to distinguish between the two.

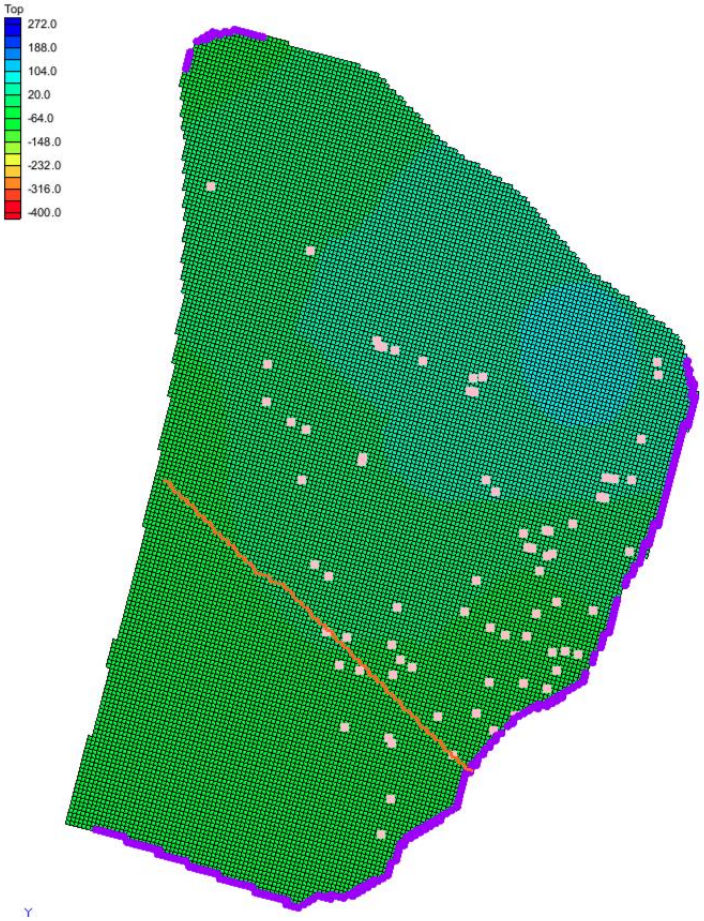

Figure 5. Model Layer 2 with Elevation Shading, Transient Boundary in Purple, Fault in Orange, Wells in Pink

The Oceano fault (in orange in Figure 5) causes a vertical offset at the lower contact, with contact elevations south of the fault approximately 370 feet higher than the northern contact (Cleath & Associates, 1996). This offset can be seen in the cross section L-L' in Figure 6. Cross Section L-L' from Fugro 2015 which runs north to south down the coastline.

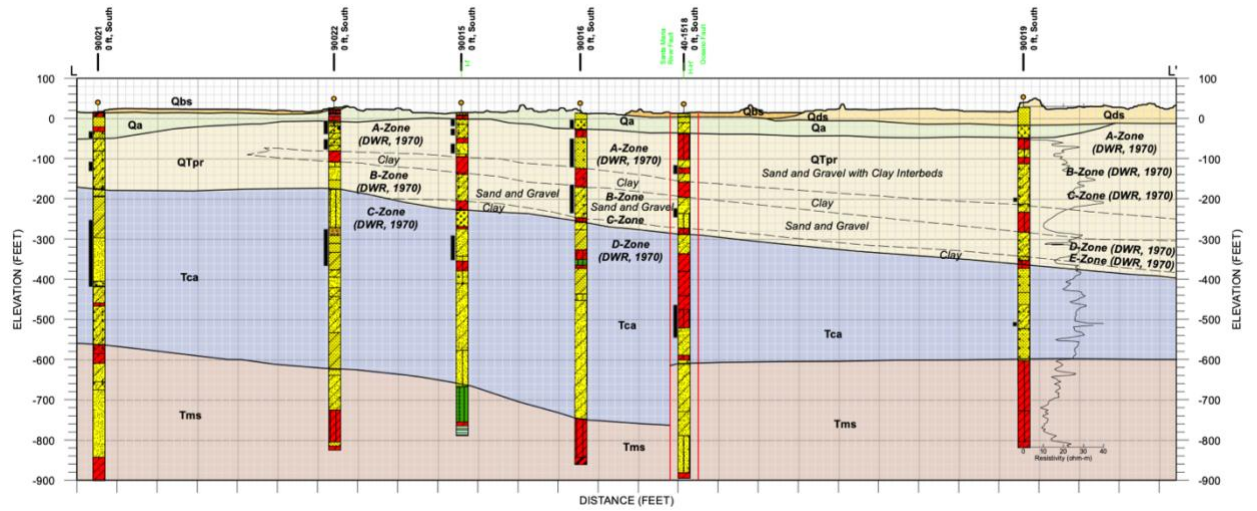

Figure 6. Cross Section L-L' from Fugro 2015

Both this layer and the third layer grid elevations were interpolated from three cross sections (H, I, & L) from the Santa Maria Groundwater Basin Characterization report (Fugro Consultants, Inc., 2015) and were modeled as confined layers.

2.2.3. Bottom Layer

The bottom layer (Layer 3), the Careaga Formation, also ranges from 150 to 700 feet thick but is comprised of two unique units: the upper Graciosa member and the lower Cebada member. Soils for both members are fine to coarse grained sand, gravel, silty sand, silt and clay, with the lower member (Cebada) being finer grained than the upper. The Careaga is of marine origin with shells distributed throughout the formation (Fugro Consultants, Inc., 2015). The Careaga Formation is also offset by the Oceano Fault (in orange in Figure 7), although the magnitude has not been well documented.

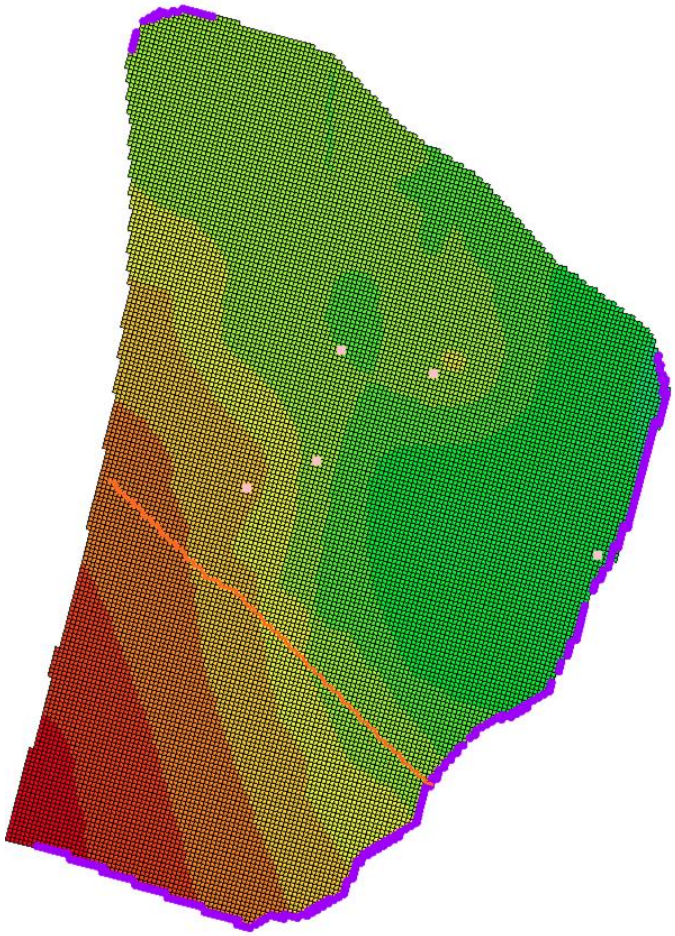

Figure 7. Model Layer 3 with Elevation Shading, Transient Boundary in Purple, Fault in Orange, Wells in Pink

Some portions of the model are underlain by the Sisquoc Formation which also has two main units: a fine grained unit of diatomaceous and porcelaneous mudstone and claystone; and a coarse grained unit of fine to coarse sandstone and siltstone. This formation has been shown to have very low specific capacity, less than 0.1 gpm/ft^2, and is considered insignificant in terms of yield for water wells (Fugro Consultants, Inc., 2015). For this reason, the Sisquoc Formation was grouped into the surrounding bedrock.

2.3. Layer Hydraulic Properties

The model required hydraulic conductivities, horizontal and vertical anisotropy, specific yields and specific storages.

Hydraulic conductivity (*K*) describes a material's capacity to transmit water. Hydraulic conductivities for the different layers and formations have been studied multiple times through pumping tests, specific capacity tests and soil profiling. Some of these various horizontal hydraulic (*HK*) conductivities are shown in Table 1. Initial horizontal hydraulic conductivities representing approximate midpoints of previous studies (Table 1) were chosen as 80, 115, and 9.5 ft/day for Layer 1, 2, and 3 respectively.

Table 1. Summary of Horizontal Hydraulic Conductivities from Previous Studies

Layer	Name	NCMA (Todd, 2007)	DWR 1970	DWR 2002	Worts 1951	Fugro 2015	Fugro 2018	Wallace 2016
1	Alluvium	27	110-400	95-400	-	270-600	-	15
1	Old Dune Sand	47	-	-	-	175	-	52
2	Paso Robles Formation	13	70-230	15-360	-	2-15	115-270	15
3	Careaga Formation	7	-	-	9	-	12-13	3

Vertical anisotropy is the ratio of horizontal (*HK or* k_h) to vertical (*VK or* k_v) conductivity. This metric can vary by magnitudes with very homogenous (isotropic) soils close to 1 and very anisotropic soils, like clay, sometimes exceeding 100 (Duffield, 2019). A typical vertical anisotropy (VANI) of 10 was used as an initial starting point.

Specific Yield (S_y) is a dimensionless metric used to describe the volume of water released from an unconfined aquifer per unit surface area per unit decline of the water table. The Central Coast Blue Technical Memorandum 3, Figure 18, describes the specific yield for Layer 1 as approximately 0.13 (GEOSCIENCE, 2019).

Specific Storage (*SS*) is the volume of water that a unit volume of a confined aquifer releases from storage under a unit decline in head. This parameter depends on the compressibility of the water and aquifer. Specific storage was estimated from the Central Coast Blue Technical Memorandum 3, Figure 19, with values of 0.00075, 0.00025, and 0.000001 ft^{-1} for layers 1, 2, and 3 respectively (GEOSCIENCE, 2019). Specific storage was a required field for layer 1 since it is classified as convertible, which can have confined areas, even though layer 1 is unconfined.

2.4. Streams

The model has the Arroyo Grande Creek running through it and terminating into the Pacific Ocean (shown in aqua in Figure 4). This creek was traced from the map with stage data provided by Erik Cadaret from Water Systems Consulting for two stream gauge stations: Arroyo Grande Creek (upstream) and 22nd Street Bridge (downstream).

Streamflow at the Arroyo Grande stream gauge was calculated via the Manning's Equation (Equation 1) with a slope of 0.0132, roughness of 0.035, area equal to width times gauge height, and a wide rectangular channel assumption allowing R to be equal to the width. Manning's roughness, *n*, was estimated as 0.035 from the classification of "Normal Main Channel- straight, no rifts or deep pools, with stones and weeds" (Corvallis Forestry Research Community, 2021). Widths were estimated from the ruler tool in google earth at cross sections at the respective stream gauge locations. Slope was

estimated by MODFLOW from the change in elevation between the three nodes (the two gauges and terminus with the ocean) and the distance between each. The slope corresponding to the upstream, Arroyo Grande, gauge was used in the calculation.

$$V = \left(\frac{1.49}{n}\right) AR^{2/3}\sqrt{S} \qquad \textit{(Equation 1)}$$

Where,

V is the streamflow (ft^3/day)

n is the Manning's Roughness for an open channel

A is the cross sectional area (ft^2)

R is the hydraulic radius (ft)

S is the longitudinal slope (ft/ft)

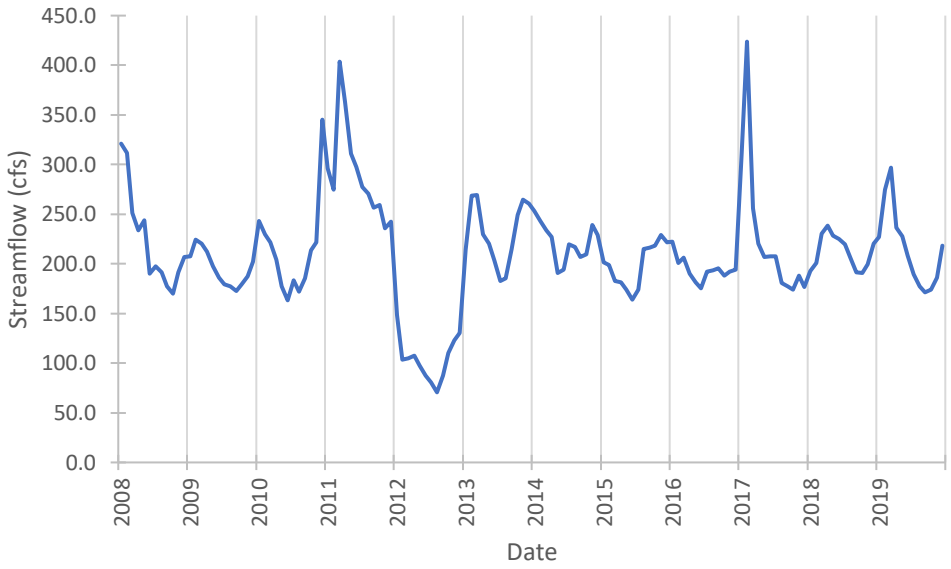

Figure 8. Streamflow from Arroyo Grande Creek Stream Gauge

The DWR 2002 report estimates typical streamflow losses above the 22nd Street Bridge gauge ranging from 1.7 to 5 cubic feet per second with a general infiltration estimate of 10% of streamflow (Department of Water Resources, 2002). The stream flows through Corducci and Typic Xerofluvents soils which are categorized as

Hydrological Soil Group A, i.e., high drainage potential. Streambed thickness is unknown, so a value of 3.28 ft (1 m) was used, similar to the value in the USGS Open File Report on the streamflow package (USGS, 2004).

With the respective widths (*w*, ft), average soil hydraulic conductivities (*k*, ft/day) (Table 2), and streambed thickness (*t*, ft), the stream conductance per unit length of a streambed (*C*, ft^2/day/ft) was estimated using the following equation.

$$C = \frac{k}{t}w \qquad \textit{(Equation 2)}$$

Table 2. Stream Characteristics at Two Gauge Stations

Stream Gauge	**Width (ft)**	**Hydraulic Conductivity (ft/day)**	**Conductance (ft^2/day/ft)**
Arroyo Grande	21	29.5	193.8
22nd Street	15	29.5	138.4

The Arroyo Grande Creek is joined by the Los Berros Creek on the eastern side of the model. However, the Los Berros Creek has very little data and is relatively small in comparison to the Arroyo Grande Creek. On the norther edge of the model is the Pismo Creek and lagoon. Very little data exists for this area also, with water level being heavily dictated by the changing dune sand at the outlet to the Pacific Ocean. This stream was modeled as a transient boundary with contour data from the NCMA reports (elaborated further in the observation well section).

2.5. Faults

Two faults exist within the NCMA model space, the Santa Maria River Fault and the Oceano Fault. A third fault, the Wilmar Fault follows Highway 101 just outside the northern boundary of the NCMA. The Wilmar Fault shows evidence of being a no flow boundary along with the outcropping of the Pismo Formation that acts as bedrock. The

Santa Maria River fault (orange in Figure 5 and Figure 6) also shows strong evidence of acting as a flow barrier in lower layers due to head differences across the fault of approximately 40 feet (GEOSCIENCE & Water Systems Consulting, 2018). Very few head observations are available for either side of the Oceano Fault, so barrier status is unknown at this point.

2.6. Recharge Rates and Areas

Recharge to the aquifer was calculated via a soil water balance. Data used for the analysis consisted of daily rainfall and reference evapotranspiration (ET_o) from the Oceano (795) CIMIS station, curve numbers for the SCS curve method, and specific crop evapotranspiration (ET_{ITRC}) values from the Cal Poly Irrigation Training & Research Center (*ITRC*) Evapotranspiration Data Tool for Zone 1 (Cal Poly Irrigation Training & Reseach Center, 2021).

Recharge for the model was split into five main categories: Truck Crops (*TC*), Turf (*TF*), Bare Ground (*BG*), Native Vegetation (*NV*), and Wetland (*WL*) (Figure 9). Urbanized land, in the Tri-Cities Mesa, was not assigned a category as recharge was assumed as zero. Agricultural land was encompassed by the Truck Crops category which contained a weighted areal average, shown in Table 3, of rotation crops (assumed as small vegetables), strawberries, nursery plants and potatoes.

Table 3. Agricultural Areas and Weighting

	Rotational Crops	**Strawberries**	**Nursery Plants**	**Potatoes**
Acres	1339	110	11	12
Weighting	0.91	0.07	0.01	0.01

Turf was used to describe irrigated vegetation such as parks, playfields, and the landscaping around the airport. Bare ground applies to much of the dune area which has a very high infiltration capacity and low runoff potential. Native vegetation in the area is a mix of natural perennial grasses, shrubs, and other dune plants. The wetlands category includes the marshland in the northern part of the model that is frequently flooded.

Figure 9. Recharge Zones in the NCMA

Curve numbers were assigned for each category to describe the amount of rainfall that would runoff. The SCS curve number method was then used to estimate the monthly runoff from rainfall for each recharge category.

Crop coefficients were developed for each category with data from the ITRC's Zone 1 monthly evapotranspiration ($ET_{c,ITRC}$) divided by the ITRC grass reference

evapotranspiration ($ET_{o,\ ITRC}$) (*(Equation 3*). Crop evapotranspiration is an evapotranspiration for certain crops based on their water requirements at different growing stages and climate conditions. The USGS defines reference evapotranspiration (ET_o) as the rate of evapotranspiration representing an "extensive surface of green grass at uniform height, actively growing, well-watered and completely shading the ground". This grass is usually ryegrass or alta fescue (Irmak & Haman, 2017).

$$K_c = {ET_{c,ITRC}}\Big/{ET_{o,ITRC}} \qquad \textit{(Equation 3)}$$

K_c was developed for three water year scenarios: dry (10.5 inches), normal (18.5 inches), or wet (32.82 inches), dependent on the amount of rainfall (October to September) (Figure 10, Figure 11, & Figure 12). These categories were specified by the Cal Poly ITRC as evapotranspiration is highly dependent on weather patterns such as rainfall and temperature (Cal Poly Irrigation Training & Reseach Center, 2021).

Monthly reference evapotranspiration (ET_o) from the CIMIS station data was multiplied by each respective category's crop coefficient (K_c) *(Equation 4*) to get the crop evapotranspiration (ET_c) representative for the area.

$$ET_c = K_c \times ET_o \qquad \textit{(Equation 4)}$$

Two exceptions to this methodology were the turf and wetland categories. The turf category was assumed similar enough to the CIMIS grass ET_o reference, so the ET_o was used as the crop evapotranspiration (ET_c) (K_c equal to 1). The wetland also assumed a constant K_c of 0.80 due to lack of available data from the ITRC for this category (Stannard, et al., 2013).

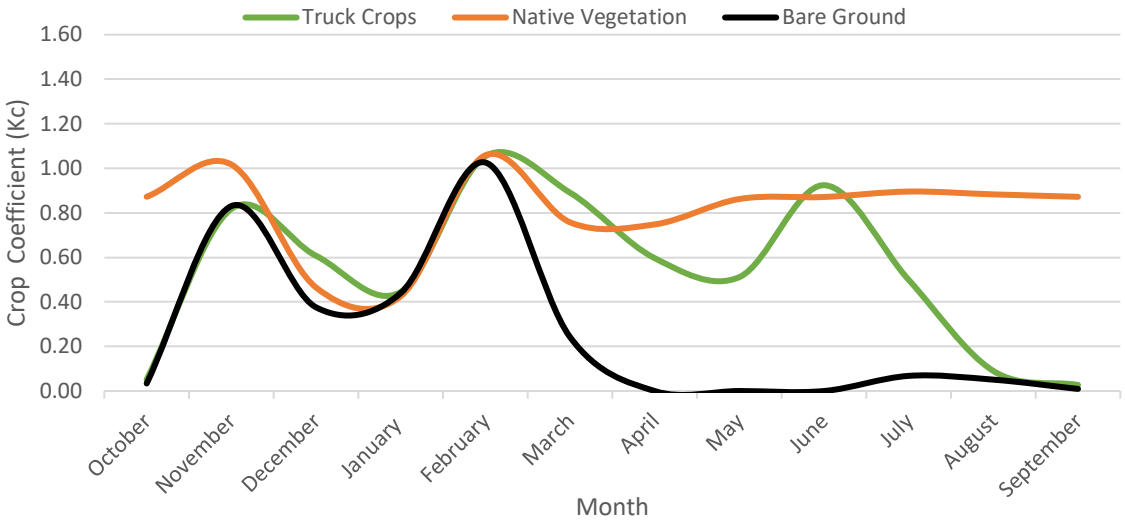

Figure 10. Monthly Crop Coefficients (K_c) for a "Dry" Water Year

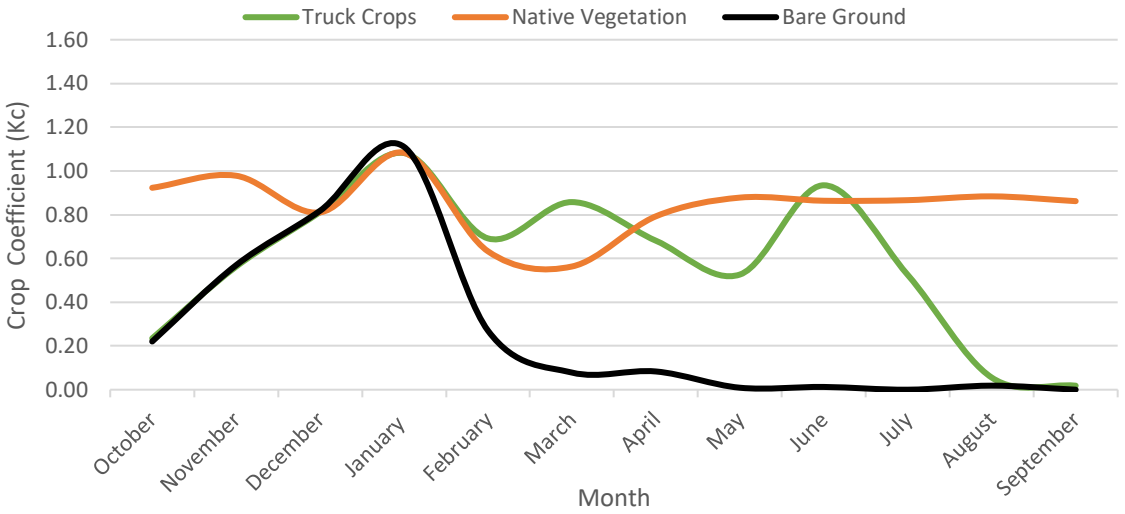

Figure 11. Monthly Crop Coefficients (K_c) for a "Typical" Water Year

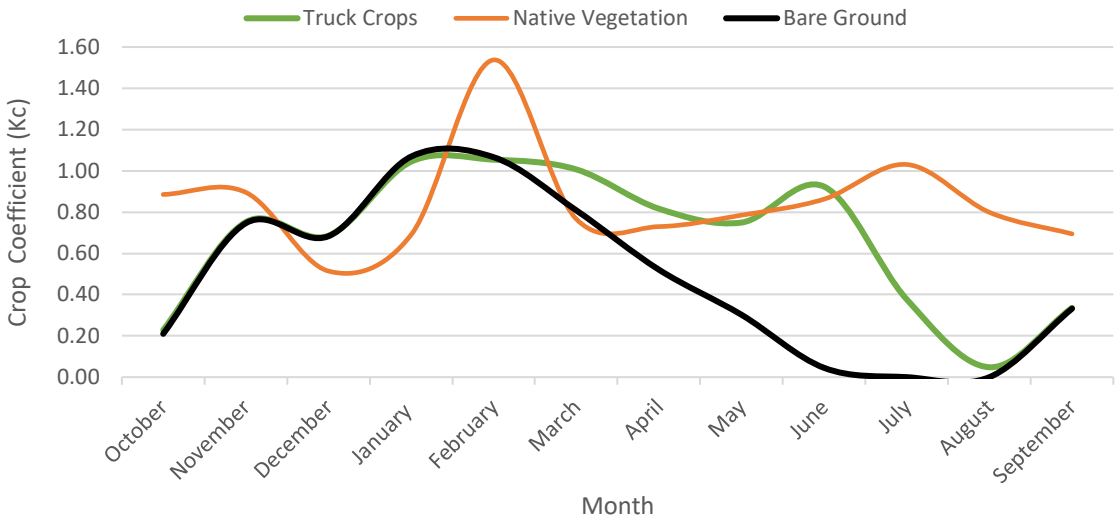

Figure 12. Monthly Crop Coefficients (K_c) for a "Wet" Water Year

Table 4. Curve Number and Average Annual Evapotranspiration (ET) for Recharge Zones

Recharge Zone Type	Curve Number	Average Annual ET (in)		
		Dry	Typical	Wet
Truck Crops	62	23.1	23.5	26.7
Turf	73	42.4	42.9	41.7
Bare Ground	49	9.5	7.3	15.8
Native Vegetation	49	35.3	36.2	35.29
Wetland	0	45.8	46.4	45.12

From there, maximum available water holding capacity, the maximum water storage in the soil, was also assigned based on soil type. Irrigation demand was derived from the crop evapotranspiration (ET_c), explained further in section 2.7, and 15% of irrigation was assumed to be lost to percolation. A water balance *(Equation 5*), was applied per month to determine the soil storage (S_{end}) from the previous month (S_{start}) , where P is rainfall (inches), and R is runoff (in).

$$S_{end} = P - R - ET + S_{start} \qquad \textit{(Equation 5)}$$

If the ending storage was greater than the available water holding capacity, then the excess was assumed to percolate along with 15% of any irrigation (Figure 13). If the ending storage for the month was below the available holding capacity, as is typical for dry months, percolation would only come from 15% of the irrigation. Soil storage was limited to a minimum of 55% of the available water holding capacity (max storage), as the moisture content in soil never drops fully to zero in practice.

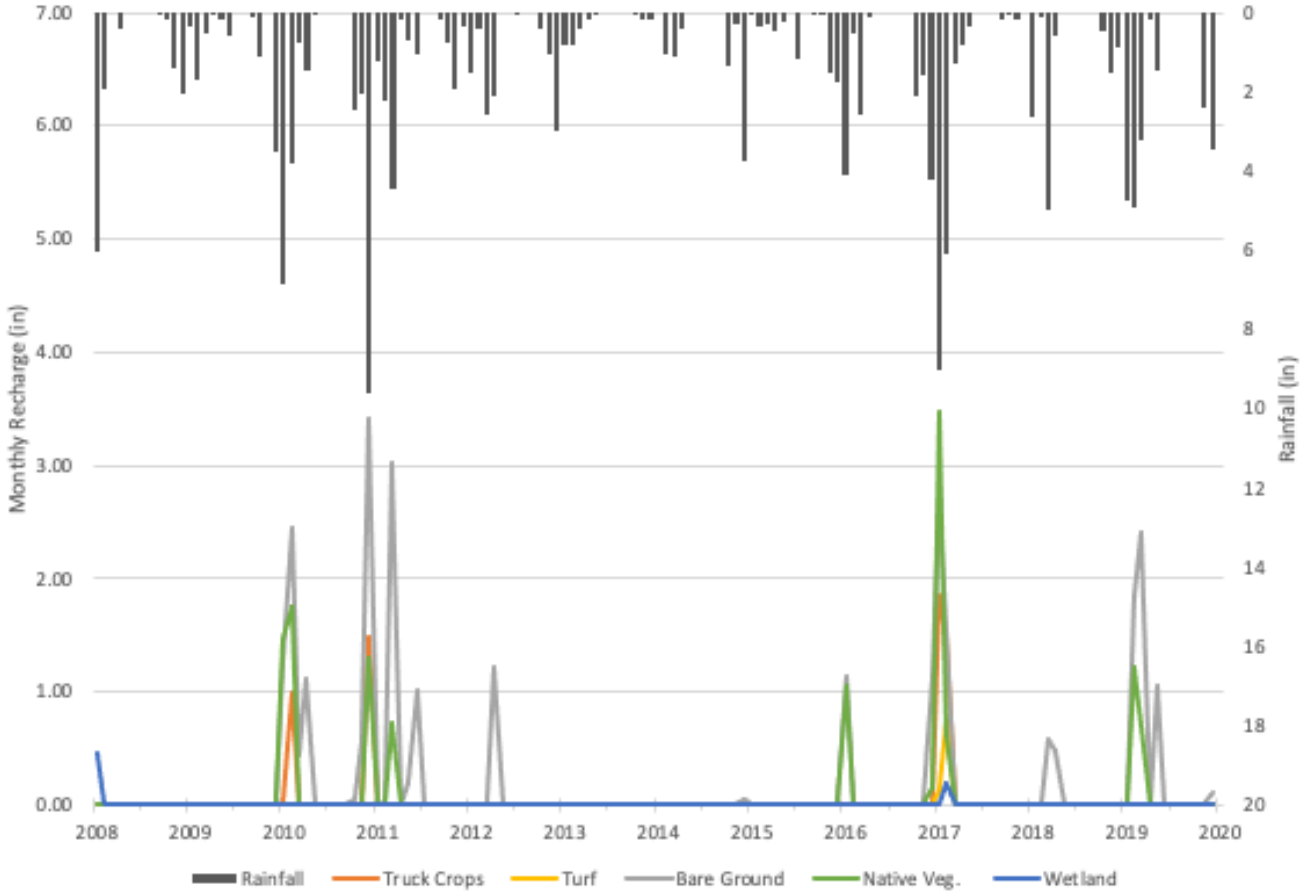

Figure 13. Rainfall (in) and Recharge (in) by Month for Different Recharge Types

2.7. Agricultural Wells

Agricultural wells are difficult to find in public databases and rarely contain pumping information. Google Earth was used to visually determine where agriculture wells may exist and estimate the approximate irrigation area each well may serve (Figure 14). This resulted in 61 irrigation wells. Screen depth was estimated by taking an average of documented wells, through well completion reports, for the area. Irrigation demand, in feet per day was estimated from the ET_c and soil moisture. When soil moisture dropped below 55% of the respective available water holding capacity for the category, irrigation would provide the difference between the available water (rainfall minus runoff) and plant water demand (ET_c). Irrigation efficiency, or the amount of water available to plants, was assumed as 85% and assumed to only maintain soil moisture from the previous month. The other 15% is assumed to contribute to percolation if available water holding capacity is met.

Figure 14. Agricultural Field Partitioning in Google Earth. Agricultural Fields in Red and Pismo Beach Golf Course in Blue

Agricultural pumping demand (ft/day) from the soil water balance previously described was multiplied by the size of the adjacent fields (ft^2) to estimate the pumping rate (ft^3/day). Approximately 1,346 acres of agricultural land was modeled. Turf irrigation pumping was only estimated for the Pismo Beach Golf course as all other turf areas (City Parks) were assumed to be irrigated by nearby municipal wells.

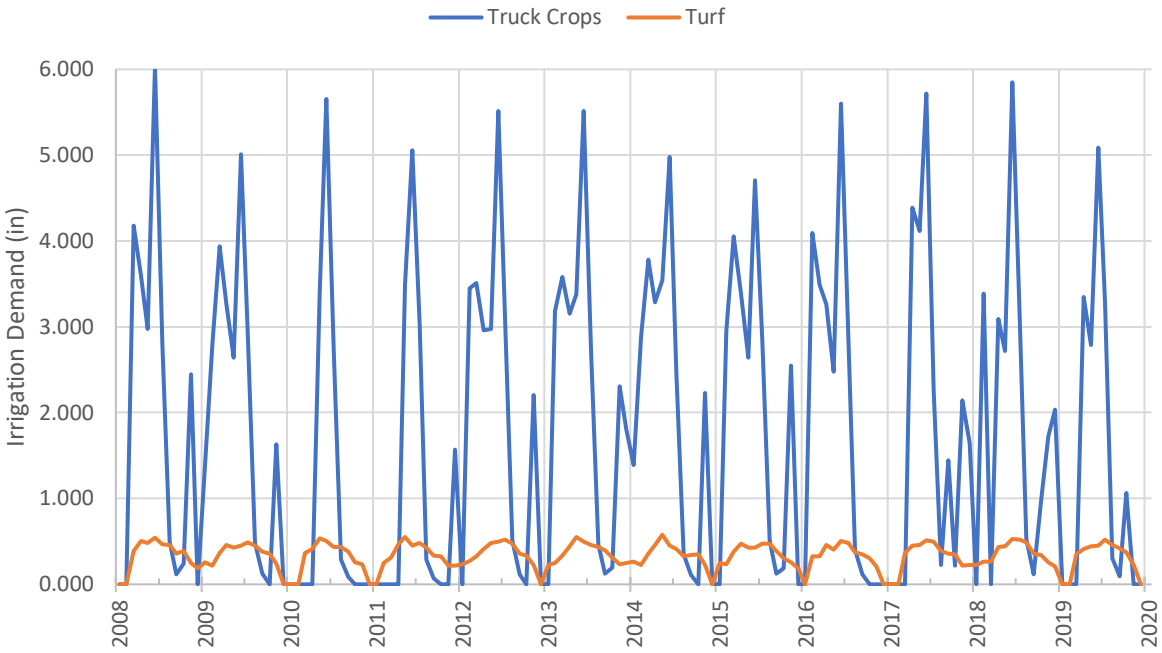

Figure 15. Monthly Total Pumping Demand (in) by Type

The annual totals were compared to the Central Coast Blue (CCB) Phase 1B Agricultural Pumping Estimates Technical Memorandum value in Table 5 (GEOSCIENCE, 2018). While the technical memorandum was prepared using the same method as this report, their approach was more detailed in terms of crop type and evapotranspiration estimation. Average percent difference from 2008 to 2016, the available data, was 2%, although large variations exist.

Table 5. Agricultural Irrigation Comparison to Central Coast Blue Technical Memorandum

Year	Modeled Ag. Irrigation (Acre-ft)	CCB Phase 1B Ag. Irrigation (Acre-ft)	Percent Difference
2008	2,567	2,457	4%
2009	2,718	2,729	0%
2010	1,364	1,547	-12%
2011	1,515	2,004	-24%
2012	2,731	2,292	19%
2013	2,967	3,277	-9%

Year	Modeled Ag. Irrigation (Acre-ft)	CCB Phase 1B Ag. Irrigation (Acre-ft)	Percent Difference
2014	2,807	3,047	-8%
2015	2,687	1,825	47%
2016	2,504	2,425	3%
2017	2,486	-	-
2018	2,641	-	-
2019	1,792	-	-

Due to the large amount of agricultural irrigation, much more than municipal (Figure 17), the variation from the more detailed CCB Phase 1B technical memorandum could contributed to high residuals in the model.

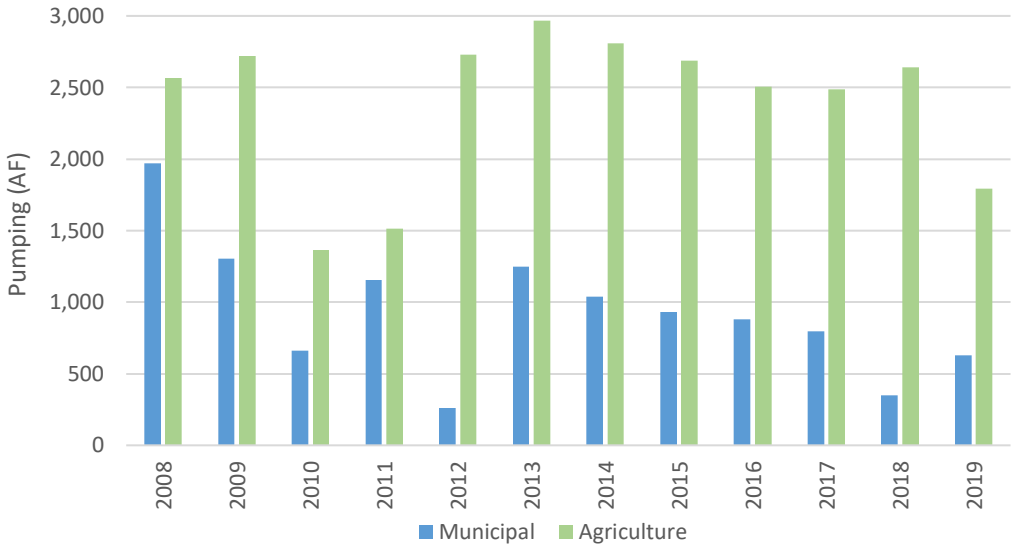

Figure 16. Comparison of Municipal to Agricultural Pumping by Year

2.8. Municipal/Domestic Wells

Municipal pumping information for Oceano Community Service District, City of Arroyo Grande, City of Pismo Beach and City of Grover Beach was provided by Nate Page from GSI Water Solutions, Inc. Turf was frequently located next to municipal wells and was assumed to receive irrigation water from these wells with the exception of Pismo

Beach Golf Course. This area had a well assigned and pumping rates determined in parallel with the agricultural method. Domestic wells do exist beyond these entities such as Pacific Dunes RV Ranch, Halcyon Water System, and Ken Mar Gardens. These small water purveyors were assumed to be minimal and were not perused due to privacy laws.

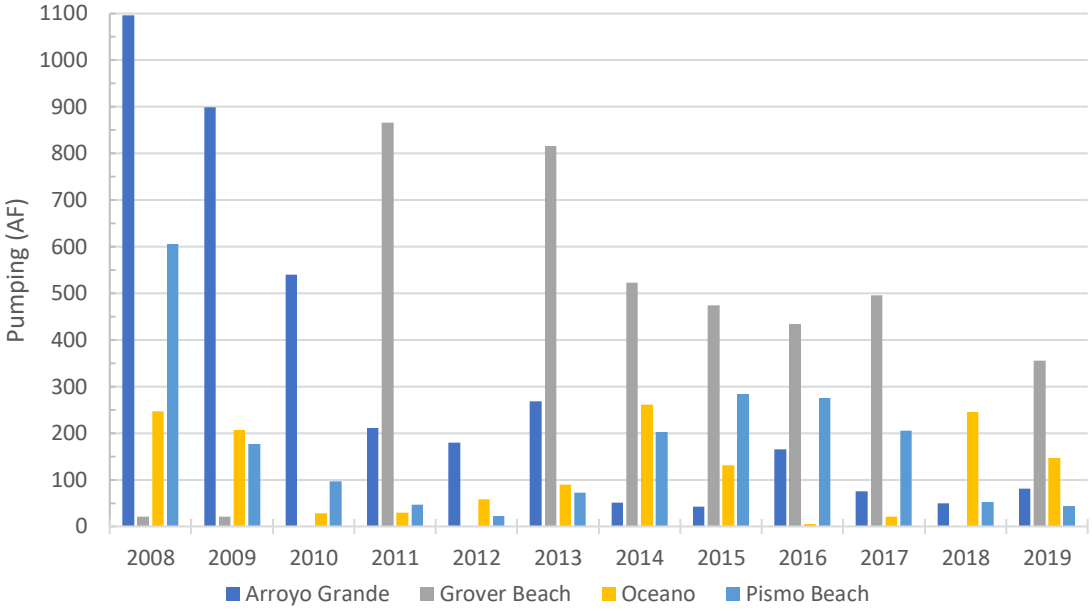

Figure 17. Municipal Annual Pumping (acre-ft) by Municipality

2.9. Observation Wells

Observation wells are wells that contain water level measurements. The County of San Luis Obispo gathers all of this data but it is not available to the public. Six observation wells were found with partial data; two from the Central Coast Blue Technical Memorandum 3, and four that had data values consistently shown in the annual NCMA reports contour maps. However, data gaps were present for each of these observation wells.

Contours, from the NCMA annual reports, were drawn in ArcMap and then rasterized. The hydraulic head values from each raster were extracted at each point where

data was missing. However, these observation wells did not have screening information available so an assumption of assigning them to layer two was made.

In addition to the observation wells are 16 Sentry wells. These hug the coastline and are sets of three to four monitoring wells at varying depths with data provided in the annual NCMA reports. They are monitored for both hydraulic head and total dissolved solids concentration to monitor saltwater intrusion.

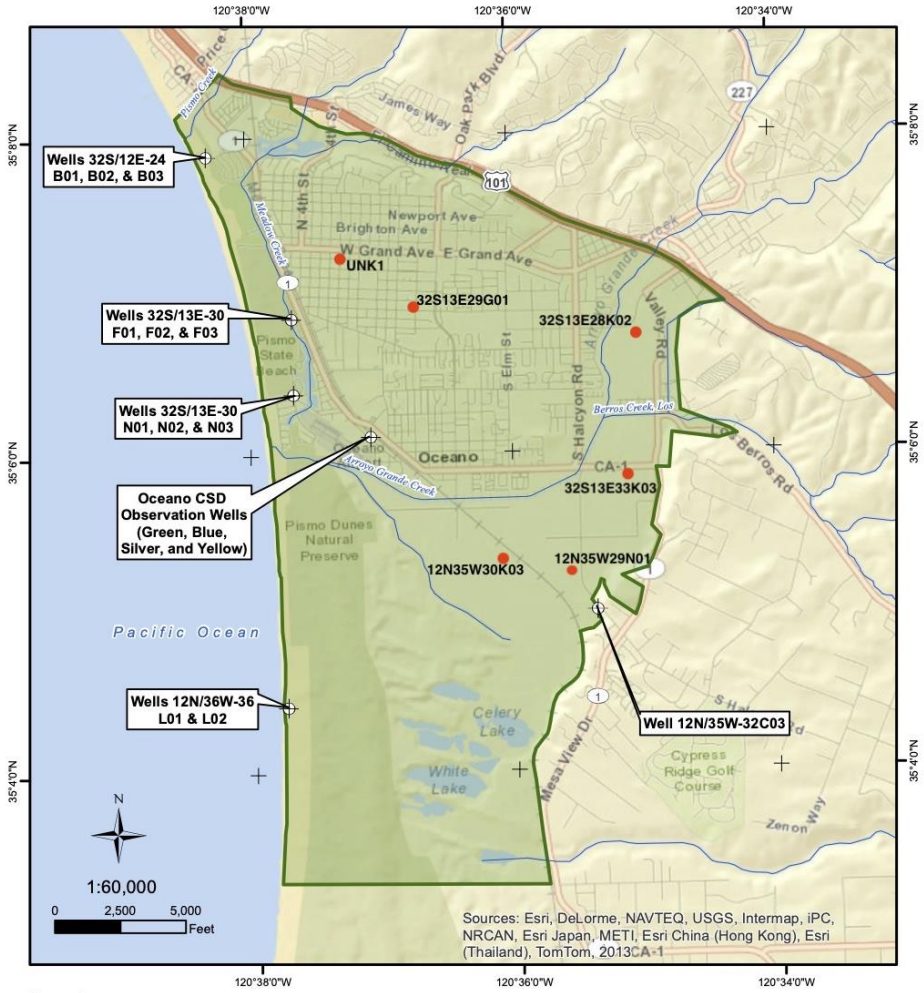

Figure 18. Sentry (white) and Monitoring (red) Well Map, adapted from Figure 7 in Fugro 2014 NCMA Annual Report

3. Groundwater Model

3.1. Background

Modeling was performed in Aquaveo's Groundwater Modeling System (GMS), version 10.4.5. GMS is a visualization platform that allows users to bring in data from a variety of sources, edit data within the program, run different modeling and transport packages, and export graphics and statistics. A conceptual model approach was used in GMS which allows GIS and other shapefile data to be imported and extracted to coverages which visually represent various components. These coverages were then mapped to MODFLOW which applies the coverage to all applicable cells, which eliminates the need to edit individual cells manually.

Within GMS, MODFLOW-NWT was used in conjunction with the Upstream Weighting (UPW) package. USGS, the developer of MODFLOW-NWT, describes it as a "Newton-Raphson formulation for MODFLOW-2005 to improve solution of unconfined groundwater-flow" (USGS, 2020). It is intended to solve unconfined aquifer problems that have drying and rewetting of cells. It builds off of MODFLOW-2005, also developed by USGS, which simulates three dimensional steady and non-steady flow in a system that can have any combination of confined or unconfined, irregularly shaped layers (USGS, 2019). MODFLOW-2005 was previously the core MODFLOW version but has recently been replaced by MODFLOW-6, however it is still maintained and supported. Both MODFLOW-2005 and MODFLOW-NWT support a variety of packages which describe various aspects of a system such as streams (STR), wells (WEL), and recharge (RCH).

However, MODFLOW-NWT differs from MODFLOW-2005 in that it must be used with Upstream Weighting (UPW) package instead of the various other intercell flow

solver packages such as Block-Centered Flow (BCF), Layer Property Flow (LPF), or Hydrogeologic-Unit Flow (HUF). Inputs for UPW are nearly identical to LPF, with the exception of all layers designated as convertible are assumed to be wettable in the UPW package (USGS, 2018). This is useful for transient models where unconfined layer cells may go dry at some point in the model but could be rewetted later on.

Both MODFLOW-2005 and MODFLOW-NWT use a finite difference equation to describe the three dimensional movement of groundwater through porous material *(Equation 6)*.

$$\frac{\partial}{\partial x}\left(K_{xx}\frac{\partial h}{\partial x}\right)+\frac{\partial}{\partial y}\left(K_{yy}\frac{\partial h}{\partial y}\right)+\frac{\partial}{\partial z}\left(K_{zz}\frac{\partial h}{\partial z}\right)+W=S_s\frac{\partial h}{\partial t} \qquad \textit{(Equation 6)}$$

Where,

K_{xx}, K_{yy}, K_{zz} are the hydraulic conductivities along the x, y, and z coordinate axis, respectively (L/T);

h is the potentiometric head (L);

W is the volumetric flux per unit volume representing sources and/or sinks of water, with W>0 for flow into the system and W<0 for flow out of the system (T^{-1});

S_s is the specific storage of the porous material (L^{-1}); and

t is time (T).

With initial head conditions and boundaries, Eq. 1 can be used to create a mathematical representation of the heterogenous and anisotropic medium, nonequilibrium groundwater flow system (Harbaugh, 2005). However, this equation is rarely simple to solve. Replacing the continuous system in Eq. 1 with a finite set of discrete points, or cells, and replacing the partial derivatives with the difference in head at the points leads to a system of linear algebraic difference equations which yield values of head at specific points and time. This is called the finite-difference method which

requires continuity within the system: the sum of the flows in and out of the system must equal the rate of change in cell storage. This continuity, with the assumption that the groundwater density is constant, is given in (Equation 7). In this case, inflow to the cell is defined as positive where outflow is negative.

$$\sum Q_i = S_s \frac{\Delta h}{\Delta t} \Delta V \qquad \textit{(Equation 7)}$$

Where,

Q_i is flowrate into the cell (L^3T^{-1});

S_s is the specific storage (L^{-1})

ΔV is the volume of the cell (L3); and

Δh is the change in head (L) over a time interval of Δt (T).

Equation 7 is computed within each user-defined cell along at each stress period. Stress periods are also user defined and help break the model simulation time into discrete periods. Variables are constant within a stress period and are allowed to change at the beginning of the subsequent stress period. Within the stress periods are time steps, with a calculated head assigned to each step. Increasing time steps can be helpful when large jumps occur between stress periods by smoothing the head vs time curves.

Predicting successive head distributions for a transient simulation requires an initial head distribution, boundary conditions, hydraulic parameters, and external stresses. MODFLOW utilizes an iterative approach to calculate these successive heads and stops iterations when convergence criteria are met (Harbaugh, 2005). However, even when a forward running model has converged, it still must be calibrated with measured data and parameters changed to produce heads that match the measured data.

Parameters can be changed manually, but this becomes incredibly complex with more than a few variables. Parameter Estimation (PEST) system, developed by John E. Doherty, can be used to automate this process with regularized inversion, using the Gauss-Marquardt-Levenberg method, to find unique values for each parameter with maximal possible accuracy (Doherty & Hunt, 2010). PEST varies the specified parameter values at each iteration to try and reduce the sum of the square residuals (Φ), where the residual is the difference between the observed and simulated data at observation points (Doherty J. , 2004).

PEST can be run with a variety of parameters and setups. The two main methods used in this method are zonal and pilot point PEST. Both methods assign a "key value" for characteristics in MODFLOW that need to be parameterized. Key values are usually large negative values that are not common in input data. PEST can then initialize these values where further specification can be made, such as initial value, minimum, and maximum values. This provides PEST with a starting point and boundaries to iterate between. An initial value far from the actual value and wide bounds can cause PEST to be unable to find a unique solution and higher error.

A parameter for a whole zone or layer can be further subdivided by using pilot points. This is a 2D Scatter Point set (or 3D in some cases) where PEST calculates the optimal parameter value at each point. The zone then has the parameter interpolated from the pilot points, giving a solution more akin to a continuous raster than piecewise zones. The downside of pilot points is that it creates hundreds to thousands more parameters than a simple zonal approach, sometimes dramatically increasing parameter estimation simulation runtimes. Pilot points can also create issues with "over fitting" and

"bullseyes", but this is mitigated by using as many well distributed pilot points as possible and editing the conceptual model if problems arise (Groundwater Modeling Decision Support Initiative, n.d.).

Each iteration of PEST has two stages: the computation of a Jacobian matrix, a matrix of all first order partial derivatives, and testing of the parameter changes. The model must be run twice for each parameter to build the Jacobian matrix, causing increased optimization time with an increase in parameters. To combat this, PEST can be run in "parallel" which allows multiple command-line windows to run the model simultaneously (Doherty J. , 2004).

An additional step to help with the many parameters created from the pilot point method is Singular Value Decomposition- Assist (SVD-Assist). This computes the Jacobian matrix only once at the beginning instead of each iteration. From this initial Jacobian matrix, SVD-Assist identifies "super parameters" based on parameter sensitivity, which is in essence a grouping of parameters. This drastically cuts down on the number of MODFLOW runs required per iteration.

3.2. Literature Review

Groundwater modeling has been around since the 1960s with large scale models becoming possible in the late 1970s (Zhou & Li, 2011). One of the first and most prevalent software is the USGS MODFLOW program. MODFLOW-NWT was created to solve drying and re-wetting conditions that MODFLOW-2005 and previous versions were unable to accurately compute. MODFLOW-NWT is also more adept for nonlinear problems stemming from nonlinear stress packages and one or more unconfined layers

with complex geologic and groundwater-surface water interaction (Hunt & Feinstein, 2012).

For example, the Walker River Basin in Nevada was modeled in MODFLOW-NWT in conjunction with the USGS Precipitation Runoff Modeling System (PRMS). Their model was designed to represent conditions from 1919 to 2007 to estimate the distribution of groundwater recharge. They also studied the movement and quality of groundwater delivered to Walker Lake to evaluate detrimental effects to fish habitat. MODFLOW-NWT was useful for this situation due to evaporation being the primary loss mechanism, causing top cells to frequently dry out. Their model was used to study four different management strategies to reduce total dissolved solids and increase Walker Lake water level in the future. (Allander, Niswonger, & Jeton, 2014).

Another study using MODFLOW-NWT was for the North Atlantic Coast Plain Aquifer system, where they used their model to assess groundwater availability and historic storage's response to previous stressors. This model spanned three states and 19 regional aquifers and utilized Parameter Estimation (PEST) system with both head and flow observations. This model had various confined and unconfined regions on the coast, similar to this study (Masterson, et al., 2016).

Parameter estimation (PEST) is not unique to MODFLOW as shown in the modeling study for five river basins in central Jutland in Denmark. Researchers used MIKE-SHE, a couple surface-subsurface model, with PEST to create a highly parameterized regional hydrological model. SVD-Assist, a PEST tool explained further in section 3.1, allowed for more flexibility in the parameter estimation process and improved head and water balance errors. The ability to process more parameters also

allowed the researchers to identify model deficiencies and inaccuracies (Danapour, Højberg, Høgh Jensen, & Stisen, 2019).

3.3. Setup

3.3.1. ArcMap

ArcMap was used for pre-processing, which included the conversion of NCMA groundwater contours to rasters, extraction of raster data to a grid of pseudo monitoring wells, and extraction of raster data to boundary arcs for the eastern and southern boundary, as well as the Pismo Creek boundary. The pseudo monitoring wells and transient boundary arcs were exported to GMS as shapefiles.

3.3.2. GMS & MODFLOW-NWT

The initial model was imported from past Cal Poly Civil Engineering graduate student Brian Wallace, who had previously built this model in MODFLOW-2005 in 2015 (Wallace, 2016). The model was brought into GMS by Dr. Muleta, however, files created outside of GMS do not import with coverages and most of the data was missing. Almost all data from the previous model was overwritten with new and extended data, however most of the original grid was preserved. Grid cells are approximately 125’ by 125’, with the grid 220 cells by 140 cells with three vertical layers. The entire model is 60,300 active cells, covering about 8,300 acres. The original grid elevations, developed from cross sections contained in Fugro Consultant’s Santa Maria Basin Characterization, were

kept with the exception of the top layer which had a new USGS 1/3 arc second DEM mapped to the ground surface.

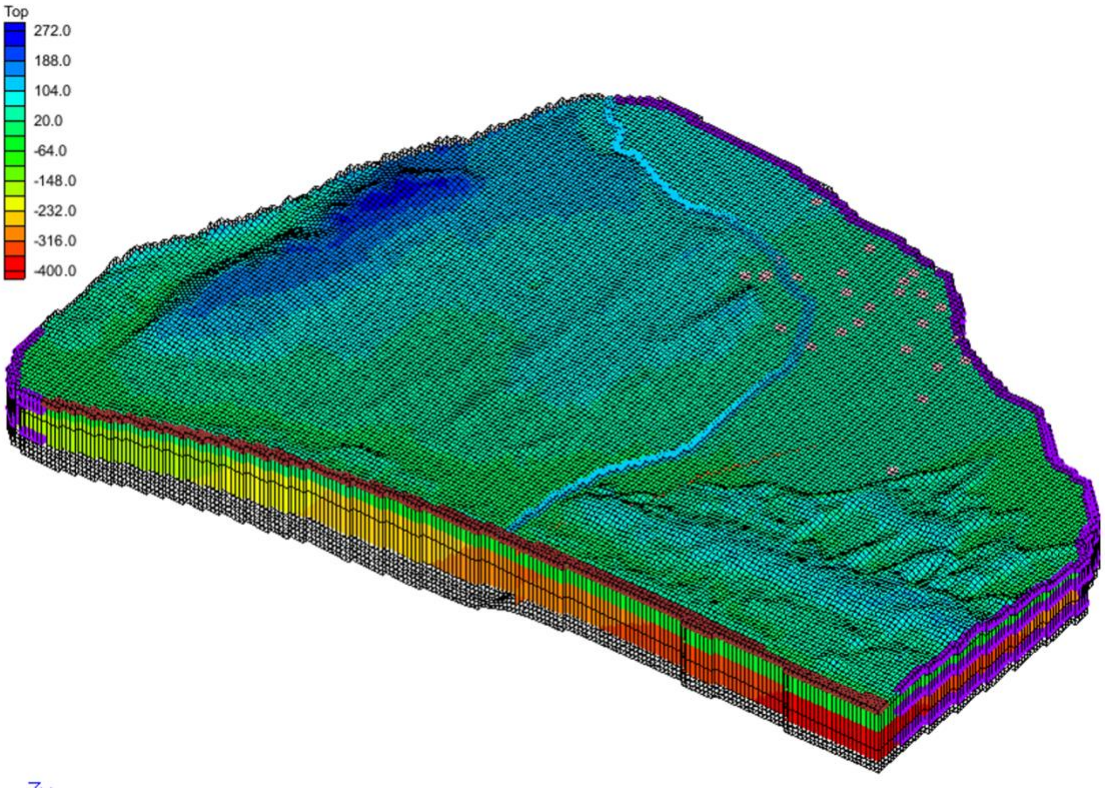

Figure 19. Model Grid Surface

GMS was then set to use a transient MODFLOW-NWT solver with the UPW package. In the UPW settings, Layer 1 was assigned as “convertible”, while Layers 2 and 3 were assigned as “confined”.

The following packages in MODFLOW were activated: General Head Boundary (GHB), Time-Variant Specified Head (CHD), Horizontal Flow Boundary (HFB), Stream (STR), Well (WEL), and Recharge (RCH). The 145 stress periods were created for each month from January 2008 to December 2019, with time steps equal to the number of days in each respective month.

The following coverages were made to reflect the data in Chapter 2 and mapped to MODFLOW: Ocean GHB, TransBound, Faults, Streams, Recharge, Irrigation Wells, Muni Wells, TransObs, and Sentry Wells.

The transient head boundaries were imported as shapefiles from ArcMap and their variable head values copied into the CHD boundary coverage at the stress periods specified by the availability of the NCMA report water head contours. When mapped to MODFLOW, the gaps between stress periods were interpolated linearly by the program. With only two observations a year for monitoring wells and up to four observations a year for Sentry wells, there are many areas with high levels of uncertainty. The CHD package assigns a head to each boundary cell both at the beginning and end of the stress period which reduces the abrupt jumps in specified head between stress periods.

While the fault coverage contained all three faults, discussed in section 2.5, only the Santa Maria had the Horizonal Flow Boundary (HFB) turned on for layers 2 and 3. A hydraulic characteristic, or hydraulic conductivity divided by width of the barrier, of zero ft/day/ft was assigned since there is documentation showing significant differences in head across the fault. However, this fault would be better modeled by creating a more representative grid frame via borehole data cross sections. However, cross sections near the eastern boundary that show the extent of the fault offset are currently lacking.

The recharge coverage was created using polygons to describe the surface use and recharge, from the soil water balance described in section 2.6, was copied in for each respective recharge zone (Figure 20).

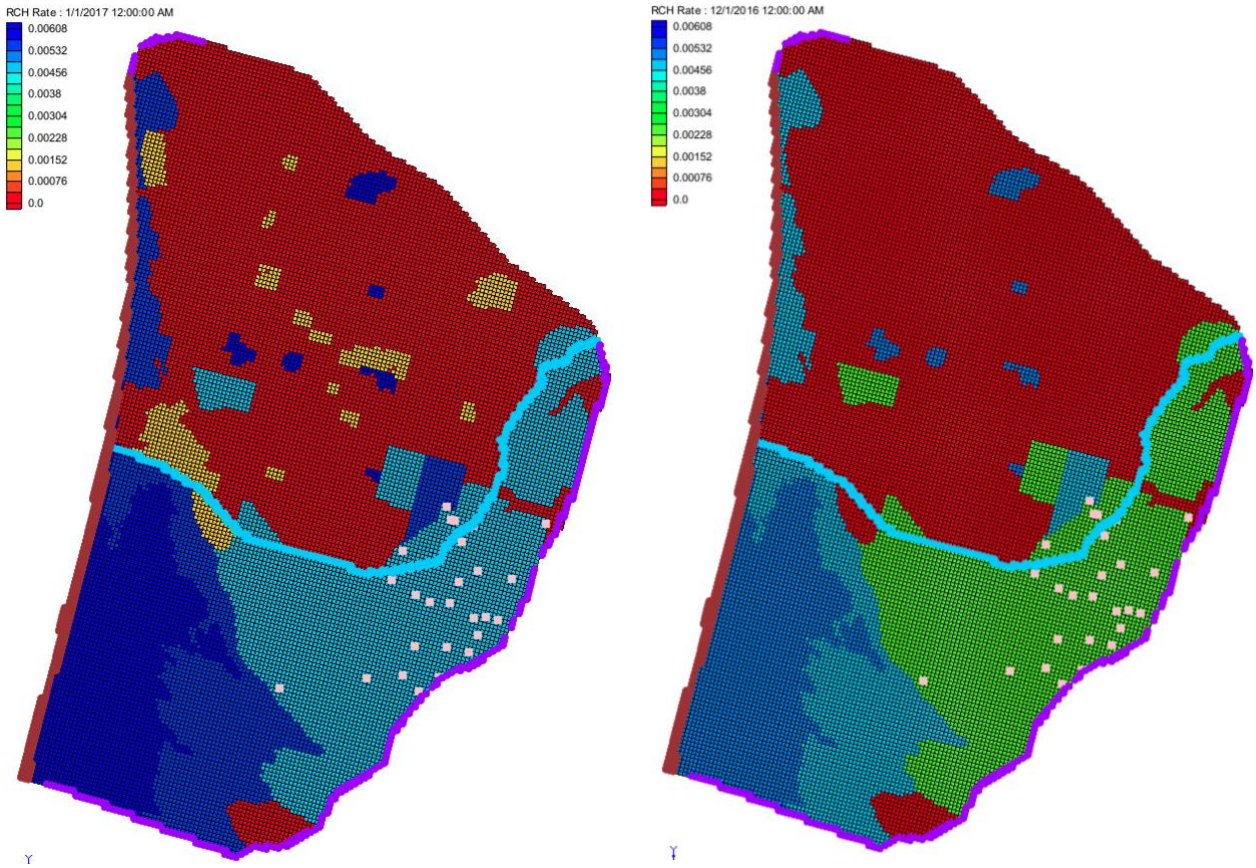

Figure 20. Grid Recharge for January 2017 (Left) and December 2016 (Right), Showing Different Recharge Zones

Irrigation wells were created in GMS by manually creating points where wells could visually be determined (assisted with Google Earth) or well logs existed. A representative well screen depth of 54 to 105 feet below ground surface was assumed based on an average irrigation well screen depth calculated from eight well completion reports in the area. This screen depth was subtracted from the surface elevation at each irrigation well to get an absolute screen elevation. Wells were mapped to MODFLOW with their layer assignment dependent on their screen depth.

The hydraulic parameters (HK, VANI, SY, and SS) were all edited within the MODFLOW dialog boxes using data identified in Section 2.3. *Sy* was not input for layers 2 and 3 due to their confinement.

Starting heads were also edited in the MODFLOW array window with October 2008 raster data, created from the 2008 NCMA annual report, used initially (described in detail in Section 2.9). The transient model was run with all other settings at the default.

While the model was able to successfully converge to a solution at each stress period, the simulated heads had a wide range of error, as is to be expected with an uncalibrated model. Figure 20 shows that the calibration targets on the Sentry wells, with heads within 1 foot of the observation in green, within 2 feet of the observation in yellow, and outside of two feet from the observation in red. The monitoring wells are in grey (as the coverage is not selected), but are all outside of the two foot tolerance and are red.

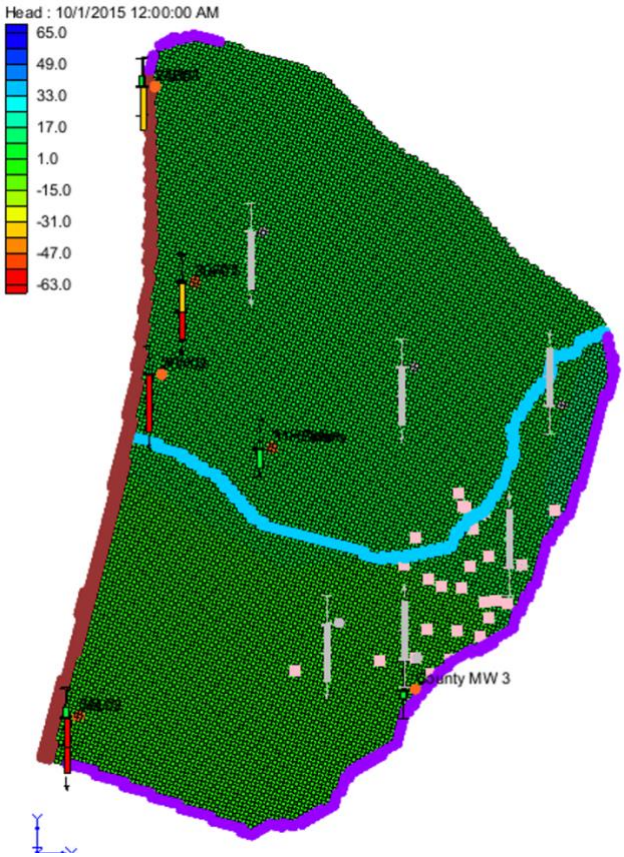

Figure 21. Layer 1 Head Shading with Error from Sentry Wells Shown

The distribution of observed vs simulated heads for all stress periods for both sets of wells is shown in Figure 22. The model seems to simulate heads that are more in line

with the Sentry wells than the monitoring wells seen by the lower degree of spread around the best fit line.

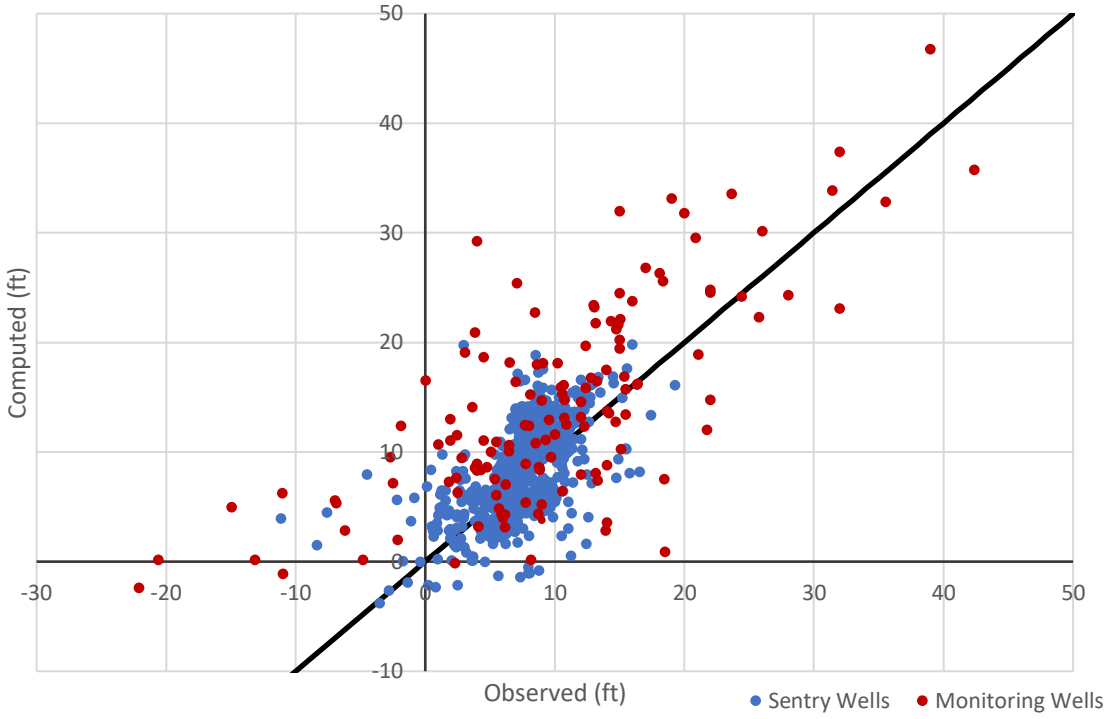

Figure 22. Observed vs Computed Head for Transient Model for all Stress Periods

Two select hydrographs are shown below in Figure 23 and Figure 24. Monitoring well 33K03 shows a very low fit between simulation data and observations. Sentry well 30F02 has an extremely low starting head and then large variations in simulation head while observations are fairly constant.

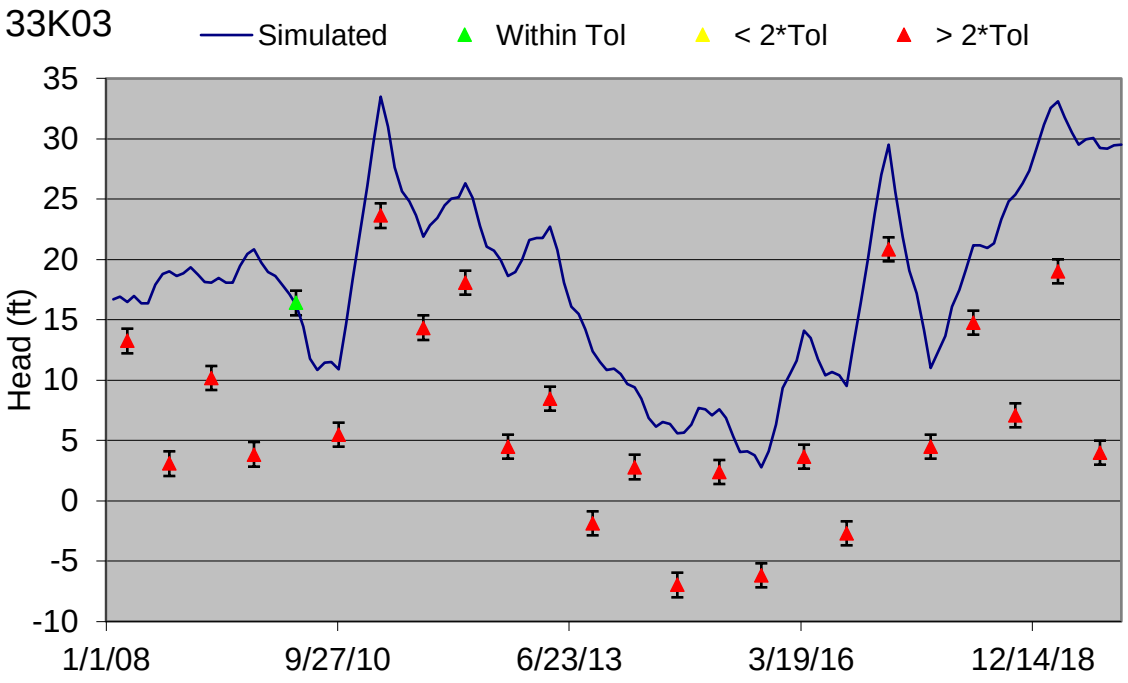

Figure 23. Hydrograph for 33K03 (Monitoring Well) Located in the Mid-Eastern Section of the Model Area

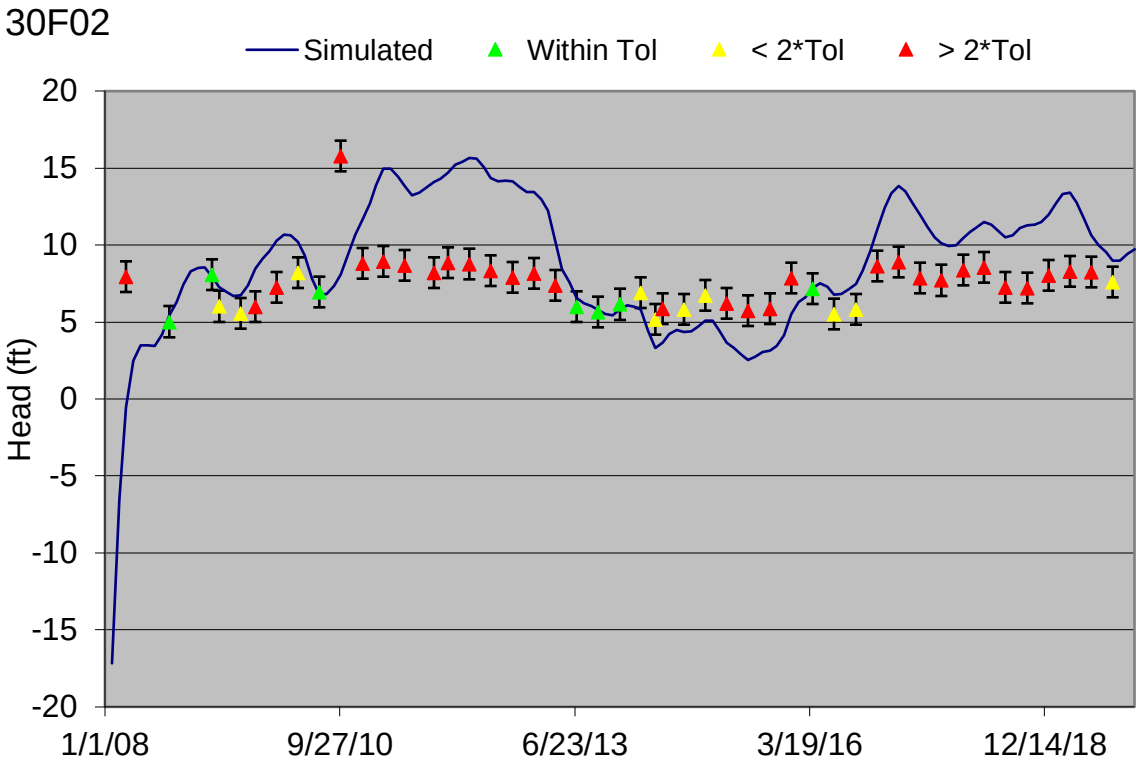

Figure 24. Hydrograph for 30F02 (Sentry Well) Located on the Upper Section of the Coast

3.3.3. Calibration

Calibration was initiated using Parallel PEST with key value parameters shown in

Table 6 and SVD-Assist enabled.

Layers 1 and 2 followed a mixed approach for parameterization with hydraulic conductivity and vertical anisotropy utilizing pilot points, while specific yield (layer 1 only) and specific storage were each parameterized for the whole respective layer. As discussed in section 2.2, layer 1 has a two main geologic units, alluvium and old dune sand. However, previous studies and compiled well pumping tests show a high variability in hydraulic conductivity within these distinct sections (Table 1). While Layer 2 is only comprised of the Paso Robles formation, there are many lenses of clay within this layer causing aquitards and perched aquifers. Pilot points allow the hydraulic conductivities and vertical anisotropies to have a range and potentially calibrate to more realistic values rather than one constant for the whole area. A set of 116 pilot points spaced approximately 2,000 feet apart was created for these variable parameters.

Other significant parameters were the conductance of the general head boundary with the ocean and the conductance of the two stream arcs. The mixed approach resulted in 473 parameters.

Table 6. Initial Parameter Values and Ranges

Parameter	Initial Value	Minimum	Maximum	Pilot Points
Layer 1 HK (ft/day)	80	47	600	Yes
Layer 1 VANI (k_h/k_z)	10	1	100	Yes
Layer 1 SY	0.13	0.01	0.3	
Layer 1 SS (ft^{-1})	0.00075	1.00E-06	0.001	
Layer 2 HK (ft/day)	115	13	360	Yes
Layer 2 VANI (k_h/k_z)	10	1	100	Yes
Layer 2 SS (ft^{-1})	0.00025	1.00E-06	0.001	
Layer 3 HK (ft/day)	9.5	4	20	
Layer 3 VANI (k_h/k_z)	10	1	100	
Layer 3 SS (ft^{-1})	0.0001	1.00E-06	0.001	
General Head Conductance ($ft^2/day/ft^2$)	0.02	1.00E-06	1	
Upstream Seg. Conductance ($ft^2/day/ft$)	193.8	1.00E-10	300	
Downstream Seg. Conductance ($ft^2/day/ft$)	138.4	1.00E-10	300	

Due to remote desktop connection concerns with the model, four successive calibration runs were completed. The four calibration runs also allowed for slight adjustments between runs to improve results, such as resetting starting head based off the first simulated stress period, adjusting boundaries, and parameters.

The first calibration run was set to 8 iterations with SVD-Assist enabled and showed sustained reduction in the Φ and reasonable estimates for parameters.

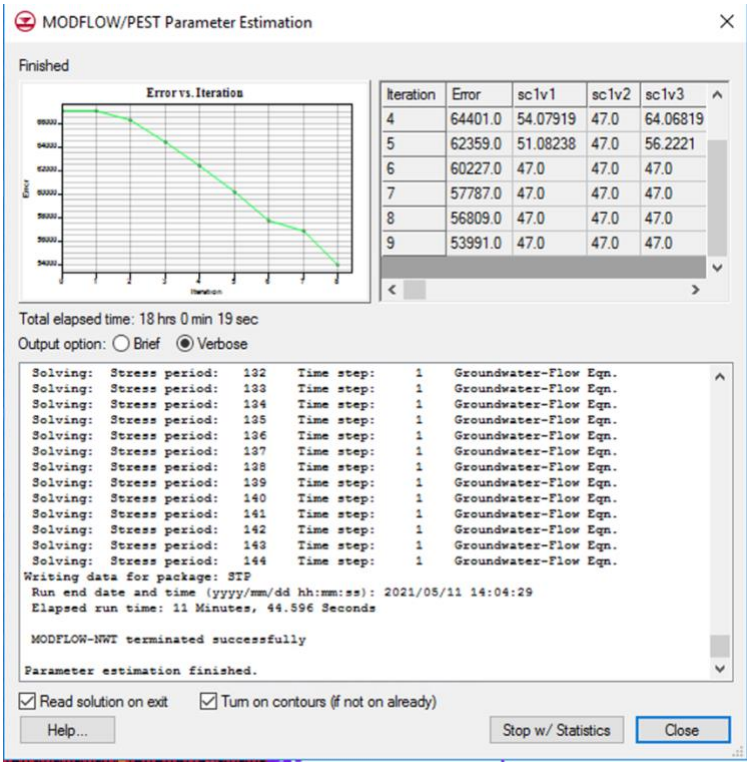

Figure 25. Calibration Run 1 PEST Dialog

Reduction in Φ for this calibration run was 16.2%. The boundary was adjusted between the first and second calibration runs, to amend a few cells that were initially missed. Simulated head at the first stress period was mapped to the starting head, and the model run in forward mode, with the re-mapping process repeated once more. This lowered the Φ by additional 8.1%.

The second calibration run was set to ten iterations with the same parameter setup as before. PEST terminated successfully, albeit a little early at seven iterations with the second run, due to low changes in parameter estimates (known as the Marquardt Lambda) between iterations. A leveling off of lambda indicates to the model that parameter estimation is finished. Reduction in Φ for this run was 1.5%.

After the second calibration run, the boundary in the lower eastern corner was adjusted to fill another gap and then PEST was run once more with a target of three

iterations. This run reduced the Φ by only 0.5%, indicating that parameter estimation was approaching the limit of its capabilities.

However, when looking at the estimated parameters from calibration run 3 (Table 7), the specific yield for the top unconfined layer was unrealistic with a value of 0.01. This value is a typical of very clayey soils which are not prevalent in this layer. The original value of 0.13 was put back into the model and run forward (no parameter estimation) to see what effect this parameter may have. Error improved indicating that this value was indeed more representative of the system and further calibration was needed. While making changes, the general head boundary for the ocean was re-evaluated. The conductance was changed using the definition described in section 2.1 to 12.4 ft^2/day/ft (from 1.0 ft^2/day/ft) to potentially be more representative.

Even with these significant changes, the fourth and final calibration run reduced the Φ by only 0.7%, indicating that neither of these parameters have a very large impact on the overall success of the model.

Hydraulic conductivities for layer 1 (Figure 26) followed expectations with higher hydraulic conductivity around the river and relatively low conductivity in the Tri-Cities Mesa and Old Dune Sand areas (West and Central). The vertical anisotropy for layer 1 is high along the coastline which is possible in the northern section considering the presence of wetlands which are commonly composed of low conductivity material such as silt or clay (Berry, Mutiti, & Hazzard, 2011). However, the high vertical anisotropy on the southern part of the coastline is unusual but could potentially be indicating poorly sorted and compacted sands in this area.

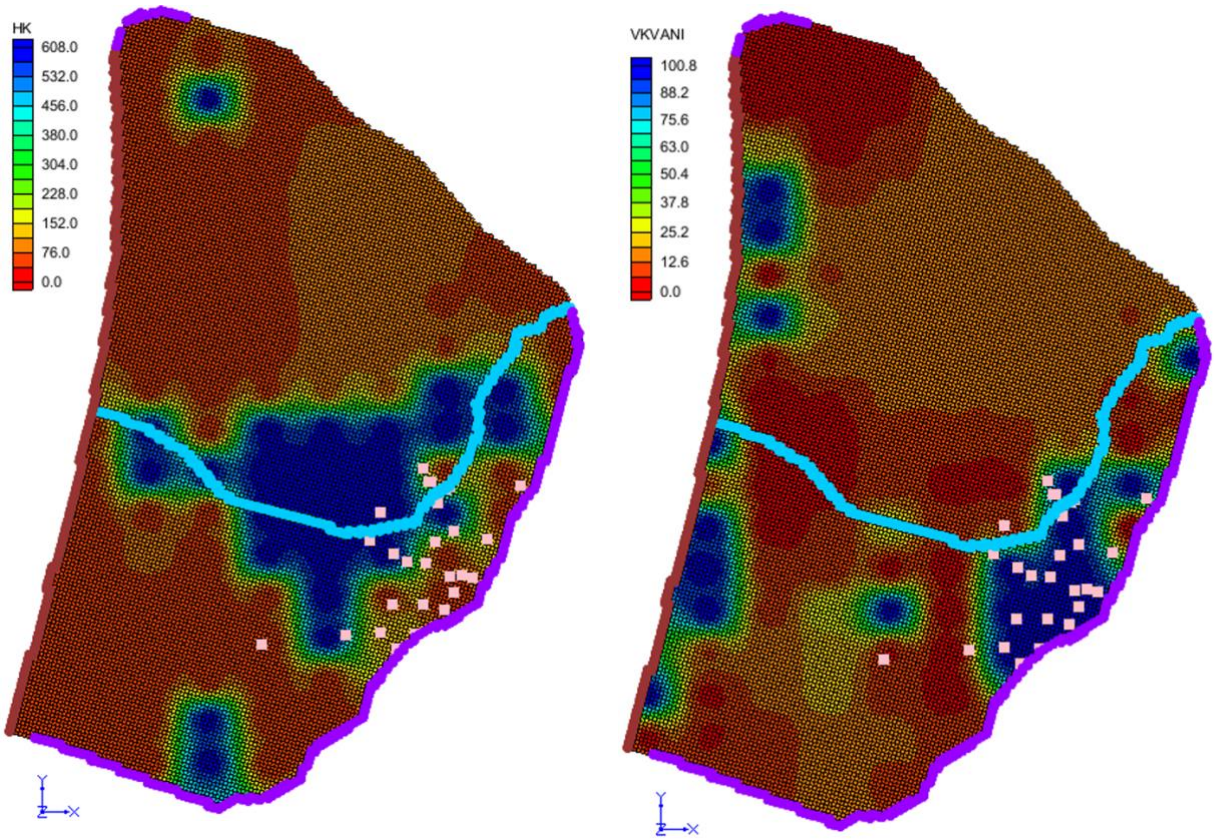

Figure 26. Calibration 3, Layer 1, Hydraulic Conductivity (Left) and Vertical Anisotropy (Right)

Layer 2 (Figure 27) shows horizontal hydraulic conductivity (360 ft/day) overall with high levels of variability that may be from a combination of factors. As discussed previously, Layer 2 is not relatively homogenous due to clay lenses scattered throughout. However, these lenses and confining layers, examined from cross sections, are more prevalent along the coast which does not necessarily match with the model's prediction. The vertical anisotropy also had a few high spots, but in this case signaling clay or another low conductivity soil. These high vertical anisotropies did seem to correspond with the areas of high vertical anisotropy in Layer 1 (Figure 26). The "bullseye effect", where sharp jumps to high or low values at pilot points, could also be at play in this layer, with the effect more pronounced in the vertical anisotropy.

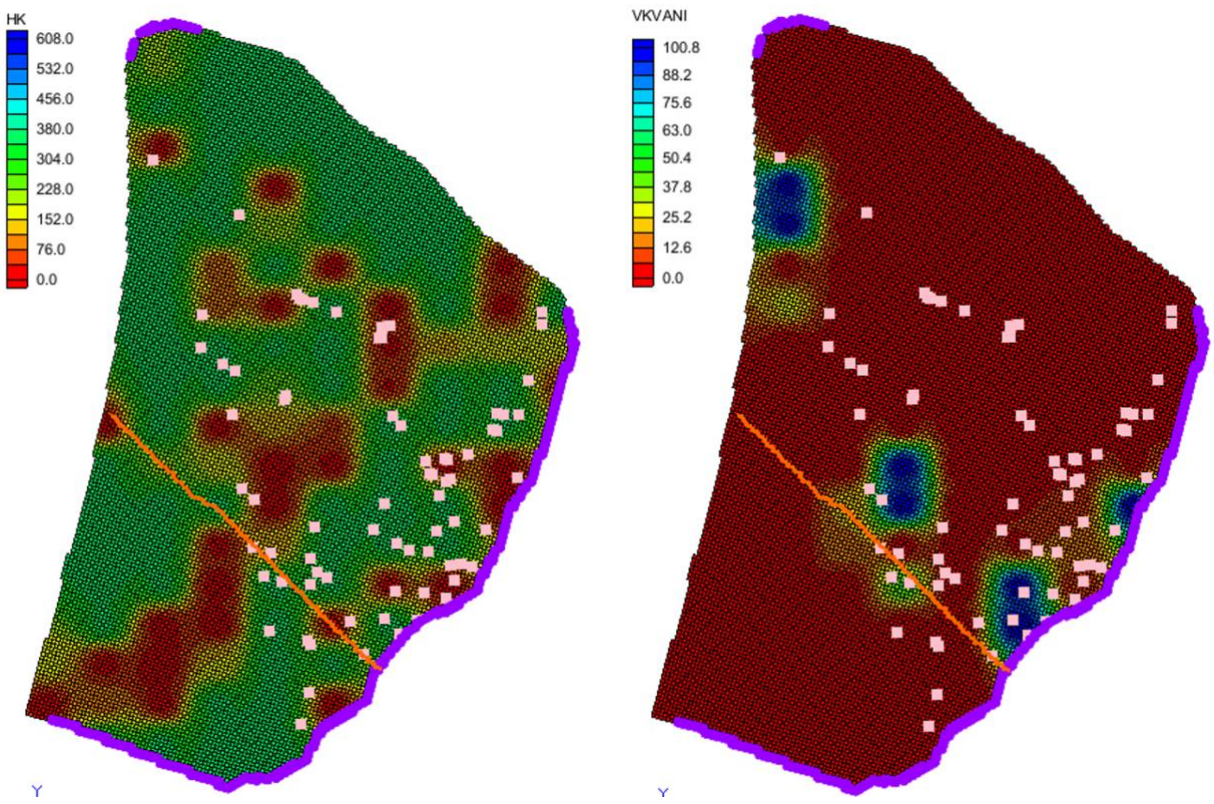

Figure 27. Calibration 3, Layer 2, Hydraulic Conductivity (Right) and Vertical Anisotropy (Left)

Results for non-pilot point parameters are shown in Table 7. Overall, the model seemed to predict reasonable Layer 3 hydraulic properties in line with previous studies but struggled with the general head boundary conductance and downstream segment conductance, with both reaching the maximum.

Table 7. Initial and Calibrated Parameter Values for All Runs

Name	Initial	Calibration 1	Calibration 2	Calibration 3	Calibration 4
Layer 1 *HK**	80	64.5	50.8	54.4	55.0
Layer 1 *VANI**	10	14.9	13.7	13.7	13.4
Layer 1 *SY*	0.13	0.00999	0.010	0.010	0.13
Layer 1 *SS* (ft^{-1})	0.00075	0.0000033	0.0000018	0.0000018	0.0000017
Layer 2 *HK**	115	360.0	360.0	360.0	360.0
Layer 2 *VANI**	10	2.9	2.7	2.6	2.5
Layer 2 *SS* (ft^{-1})	0.00025	0.0010	0.0010	0.0010	0.0010
Layer 3 *HK* (ft/day)	9.5	7.57	7.49	7.45	7.42
Layer 3 *VANI* (k_h/k_z)	10	29.5	28.8	28.3	28.1
Layer 3 *SS* (ft^{-1})	0.0001	0.00013	0.00013	0.00012	0.00012
General Head Conductance (ft^2/day/ft)	0.02	1.0	1.0	1.0	90.6
Upstream Seg. Conductance (ft^2/day/ft)	193.8	175.7	175.7	175.7	175.7
Downstream Seg. Conductance (ft^2/day/ft)	138.4	300.0	300.0	300	300

* Pilot point parameters are shown with median values

The calibrated model can be described by a variety of statistics. The correlation coefficient is one measure of goodness of fit and describes the strength of the relationship between the observed and simulated data. This metric is independent from the number of observations and a value above 0.90 is optimal (Doherty J. , 2004). The correlation coefficient from the calibrated model was 0.906, indicating an acceptable relationship between observed and simulated data.

R-squared is another useful statistic, which measures how close the data are to the line of best fit (y=x). More specifically, R-squared is the percentage of simulated head

variation that is explained by the linear model with a R-squared close to 100% (or 1) indicating that the model explains all of the variability of the simulated heads around the mean. The R-squared was calculated for the transient forward model and the calibrated model (Table 8). The calibration did increase the R-squared, although by only a nominal amount. Both R-squares indicate a less than ideal fit between the observation and simulation head.

Table 8. R-Squared Values for Transient and Calibrated Model

Observation Type	**Sentry Wells**	**Monitoring Wells**	**Combined**
Transient Model	0.33	0.53	0.45
Calibrated Model	0.36	0.59	0.50

This poor fit can be seen in Figure 28. When comparing to the pre-calibration model (Figure 22) there is a slight reduction in error with both sets of wells becoming more bunched around the residual line. However, there are still outliers in the data, especially with negative heads being overestimated. On average, the model seems to slightly overestimate with more impact to residual error with the monitoring wells.

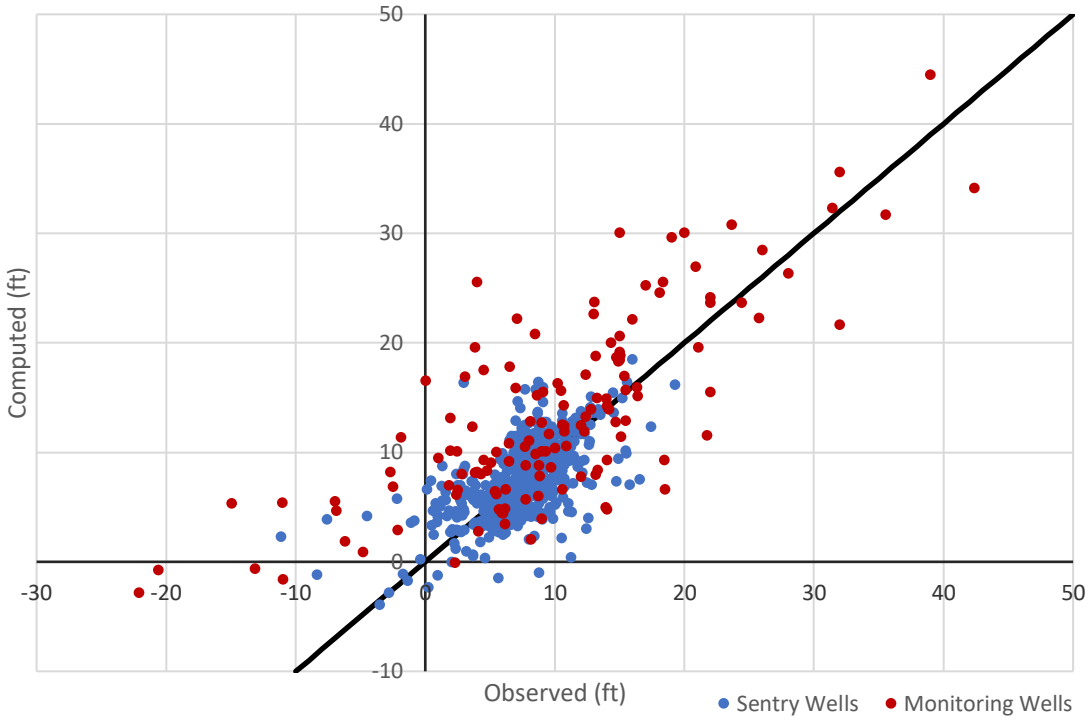

Figure 28. Observed vs Simulated Head for Calibrated Model

The same two wells from 3.3.2 are shown with hydrographs after calibration. Monitoring Well 33K03 showed no improvement with calibration and indicates that this area of the model may need further refinement. However, the general trend of the simulated head is similar to the observation data, just shifted up. Sentry well 30F02 on the other hand, improved dramatically. The model still over and under simulated in different spots but came to reduce the residuals at this well at many time steps.

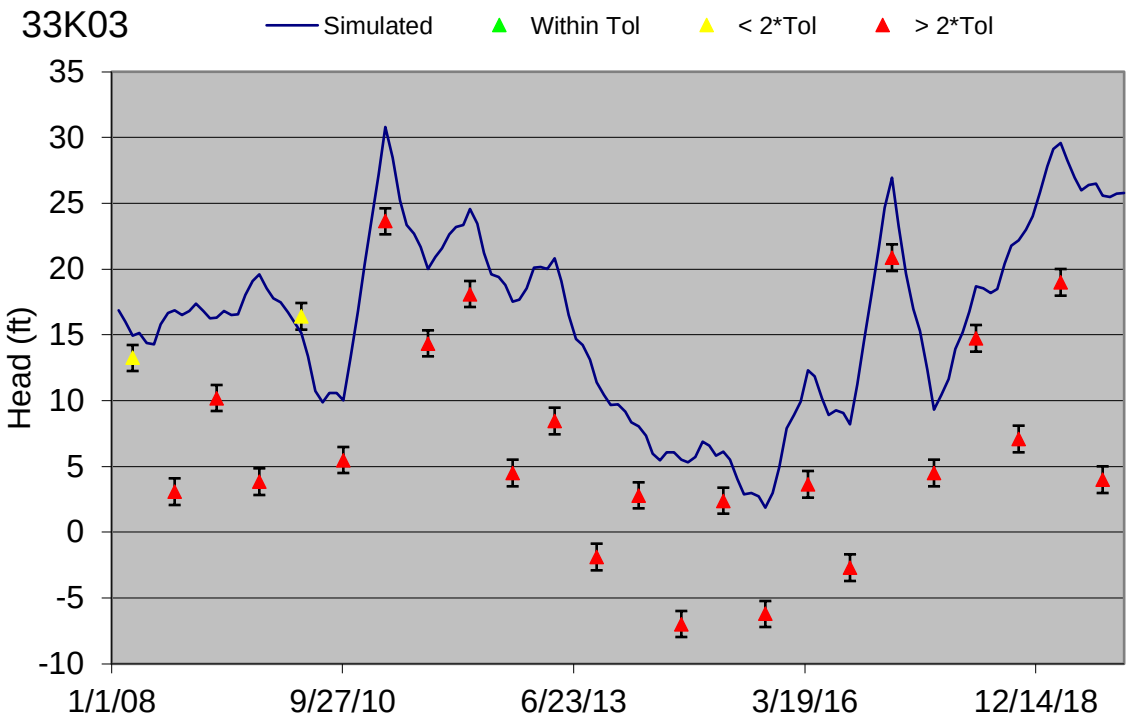

Figure 29. Hydrograph for 33K03 (Monitoring Well) After Calibration

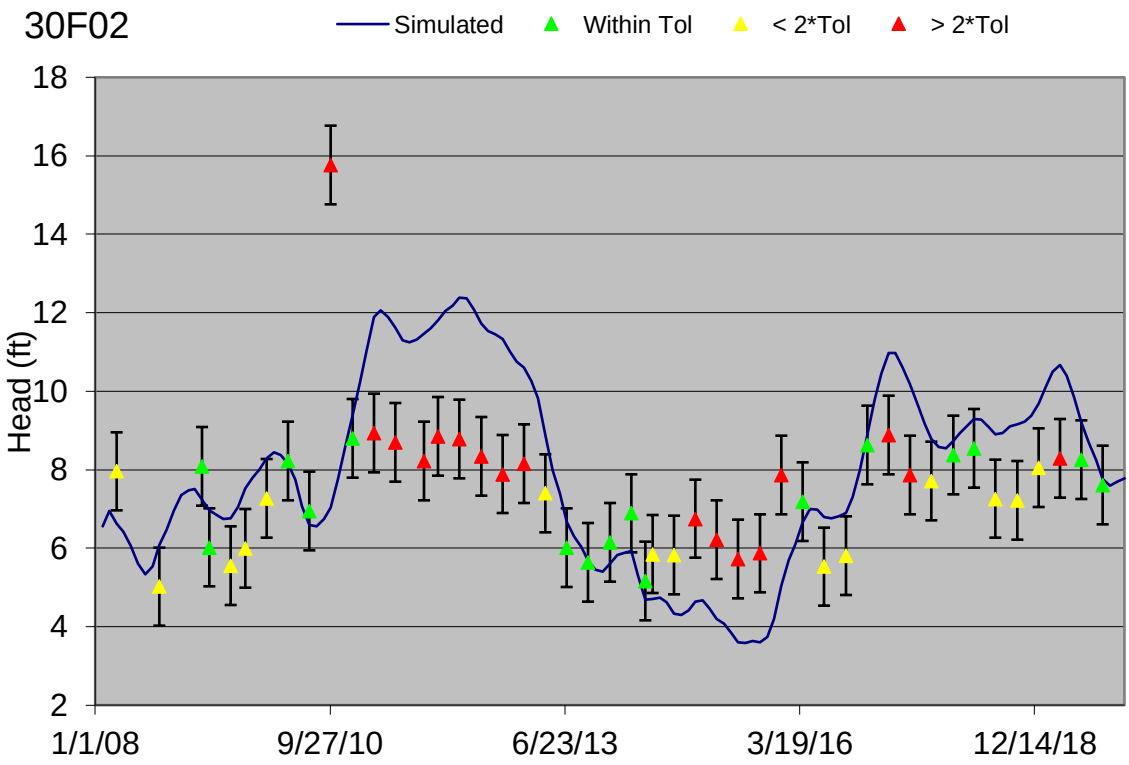

Figure 30. Hydrograph for 30F03 (Sentry Well) After Calibration

4. Results and Discussion

The results from the calibrated transient NCMA model are presented below. Analysis of results focused on comparison of the model to previous models and studies for hydrological characteristics of the three layers. In general, the lowest head conditions were observed in October of 2015 (Figure 31) and highest Heads in April of 2017 (Figure 32). Dry cells (in Red) just indicate that the hydraulic head is below the surface of that respective layer and flooded means that hydraulic head is above the top of an unconfined cell. Flooding in April 2017 was minimal, restricted to the northern wetland area and low laying agricultural area in the south. Significant shrinking of the dry zone can be seen between October 2015 and April 2017.

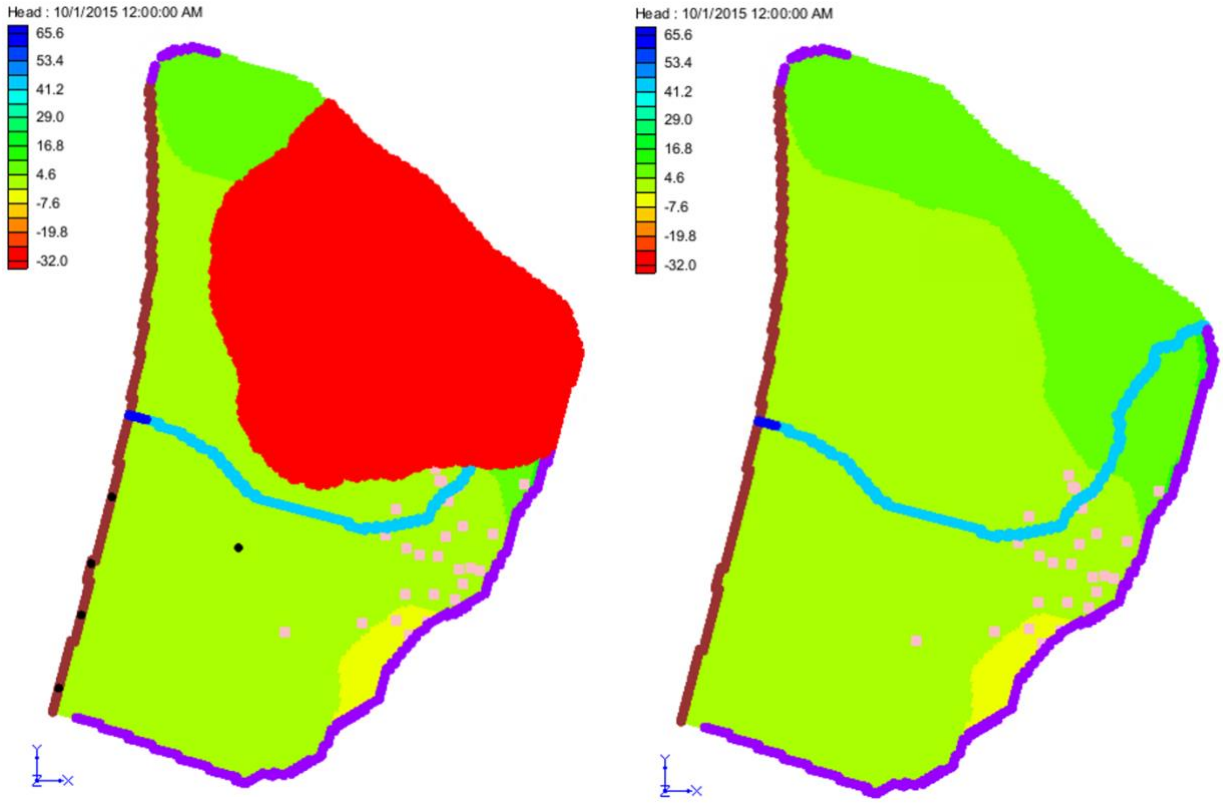

Figure 31. Heads in October 2015 in Layer 1 with Dry Cells in Red Turned on (Left) and Turned Off (Right)

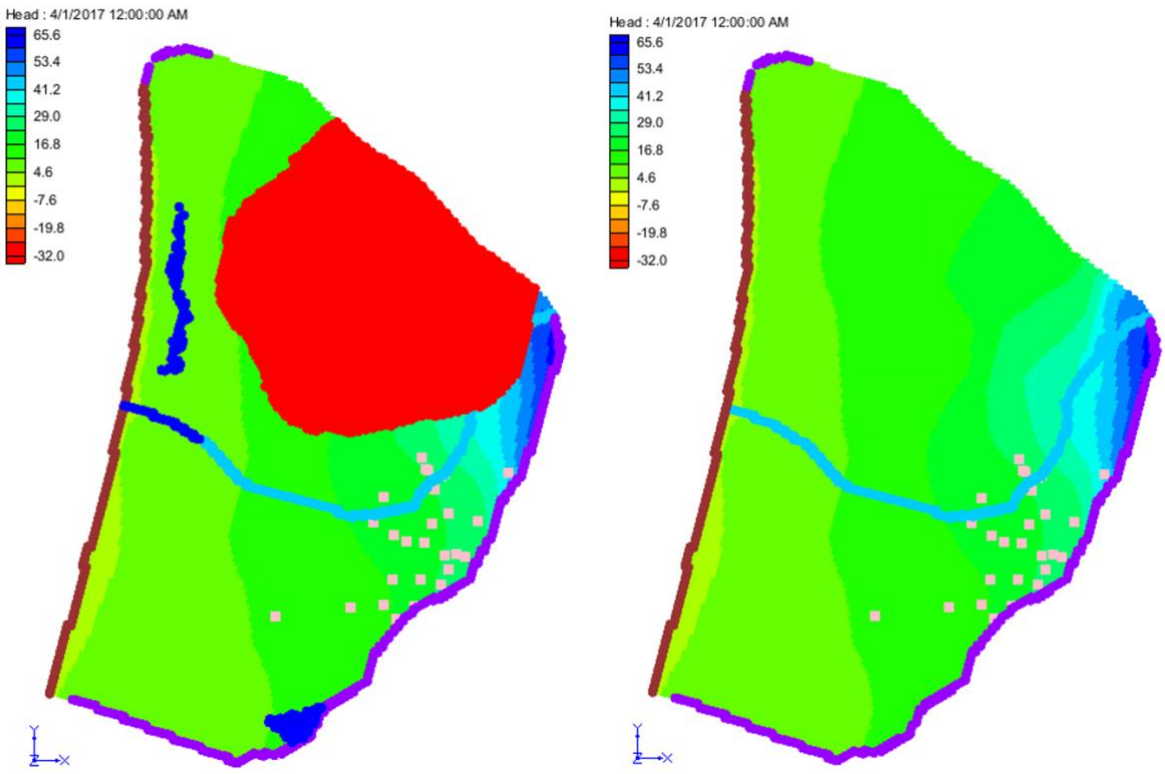

Figure 32. Heads in April 2017 in Layer 1 with Dry Cells in Red and Flooded Cells in Blue turned on (Left) and turned off (Right)

4.1. Parameters

Table 9. Final Model Parameters.
Parameters Calibrated with Pilot Points Represented by Median Value

Layer/Attribute	Name	Value
Layer 1	Hydraulic Conductivity*	55.0 ft/day
	Vertical Anisotropy *(k_h/k_z)**	13.4
	Specific Yield	0.13
	Specific Storage	0.0000017 ft^{-1}
Layer 2	Hydraulic Conductivity*	360.0 ft/day
	Vertical Anisotropy *(k_h/k_z)**	2.5
	Specific Storage	0.0010 ft^{-1}
Layer 3	Hydraulic Conductivity	7.42 ft/day
	Vertical Anisotropy *(k_h/k_z)*	28.1
	Specific Storage	0.00012 ft^{-1}
Ocean Boundary	General Head Conductance	90.6 ft^2/day/ft
Arroyo Grande Creek	Upstream Seg. Conductance	175.7 ft^2/day/ft
	Downstream Seg. Conductance	300.0 ft^2/day/ft

* Pilot point parameters are shown with median values

Final parameters are shown in Table 9 and are generally consistent with past studies. For layer 1, the range of horizontal hydraulic conductivities ranges from 47 to 600 ft/day but has a median hydraulic conductivity of 55 ft/day indicating that the majority of the top layer is on the lower end of the range. The opposite can be seen in layer 2, with the median equal to the maximum limit (360 ft/day). This pattern of a lower layer 1 and higher layer 2 horizontal hydraulic conductivity is in line with the Todd 2007 and Wallace 2016 report (Todd Engineers, 2007) (Wallace, 2016). The horizontal hydraulic conductivity estimated for layer 3, 7.42 ft/day, is between previous values of 7 ft/day (Todd Engineers, 2007) and 9 ft/day (Worts, 1951).

The vertical anisotropy (k_h/k_z) values in Table 9 for layers 1 and 2 are also medians for the range of 1-100. Anisotropy in other reports was not noted but the 2016 GEOSCIENCE Technical Memorandum 3, estimated the vertical hydraulic conductivity for layer 1 between 0.1 to 1.0 ft/day and layer 2 of 0.00005 to 1.0 ft/day. With simple division of the median hydraulic conductivity by the vertical anisotropy a median vertical hydraulic conductivity can be estimated as 4.1 and 144 ft/day for layers 1 and 2 respectively. Both values are larger than the GEOSCIENCE 2016 report and require further examination.

In terms of specific yield, layer 1 is understandably consistent with past reports as it was fixed at 0.13 before the last calibration run due to unreasonable estimations by PEST.

The specific storage was assigned to layer 1 but is inconsequential since the layer is unconfined and the low specific storage supports this. The second layer has a rather high specific storage of 0.001 ft^{-1}. This is somewhat consistent with previous literature which considers the Paso Robles Formation as the most productive of the three layers with the most storage. High specific storage is also indicative of clay, which is very prevalent in this layer, and the model seems to echo this. The bottom layer's estimated specific storage value of 0.00012 ft^{-1} indicates a sandy composition as shown by multiple reports for the Careaga Formation.

Stream conductance was not well examined in previous literature and should be explored further in future models. However, the fact that the downstream segment maxed out at 300 ft^2/day/ft indicates that the limits for iteration should be re-examined and that a high exchange between the aquifer and the stream occur in this stretch.

While the 2016 GEOSCIENCE Technical Memorandum 3 parameterized a general head boundary for the ocean interface on their top layer, the results were not shown in the published report. Based on a static distance of 125 feet from model barrier to boundary (width of a cell), an average aquifer thickness of 32 feet, and an estimated conductance of 90.6 ft^2/day per foot of boundary, the hydraulic conductivity could be 354 ft/day along this point. Of course, the distance and aquifer thickness are not static along the boundary, but this rough estimation of high hydraulic conductivity signals that the exchange along the western boundary is quite fast. This is significant as the high conductance could allow a relatively high amount of seawater inland in relatively brief stretches of inland head depressions.

The model shows the flow with velocity vectors in Figure 33 and Figure 34, with faster flow as longer arrows. Flow is generally flowing out of model into the ocean, even at the month with the lowest head conditions (October 2015). In other layers the flow occasional runs south, parallel to the coast, but never inwards.

Historical studies show groundwater gradient flowing southwest. When looking at the velocity vectors (Figure 33and Figure 34) for all stress periods, this trend mostly holds true. During wet years, like April 2017, groundwater flows more westerly with input simulated from the larger Santa Maria River Valley groundwater basin in the west. In contrast, dry years tend to recharge the greater basin and show more southernly movement.

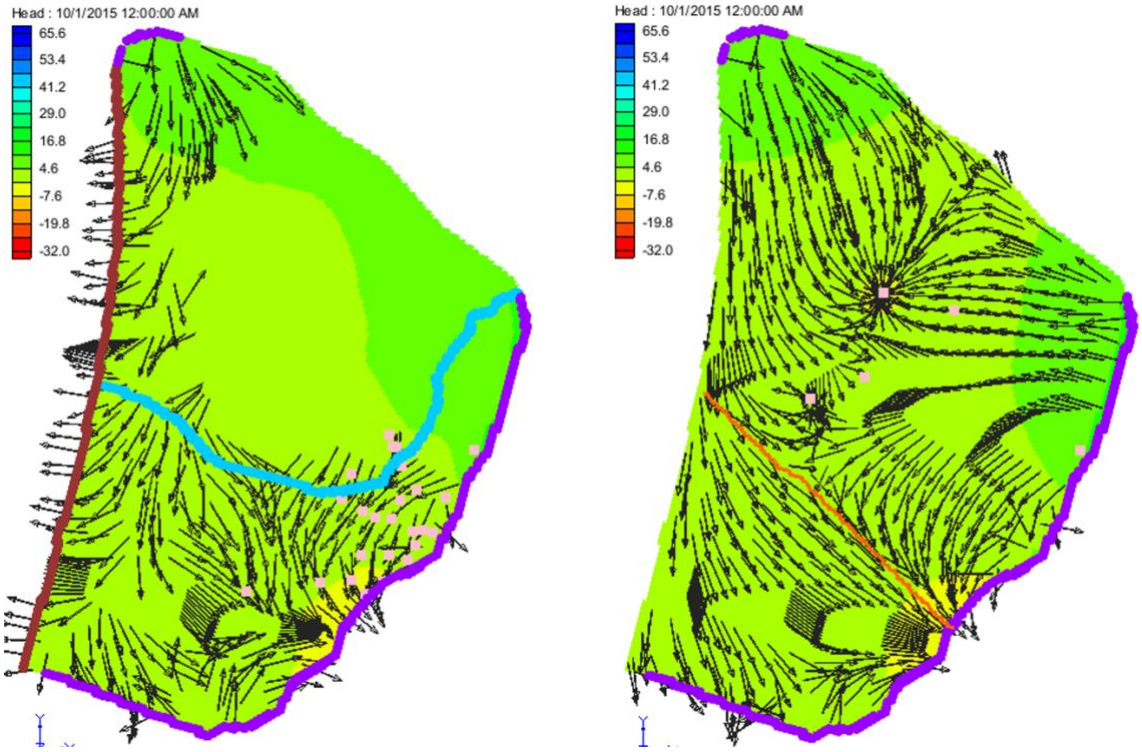

Figure 33. Head and Flow Vectors for Layer 1 (Left) and Layer 3 (Right) on 10/1/2015 (Wells as Pink Squares)

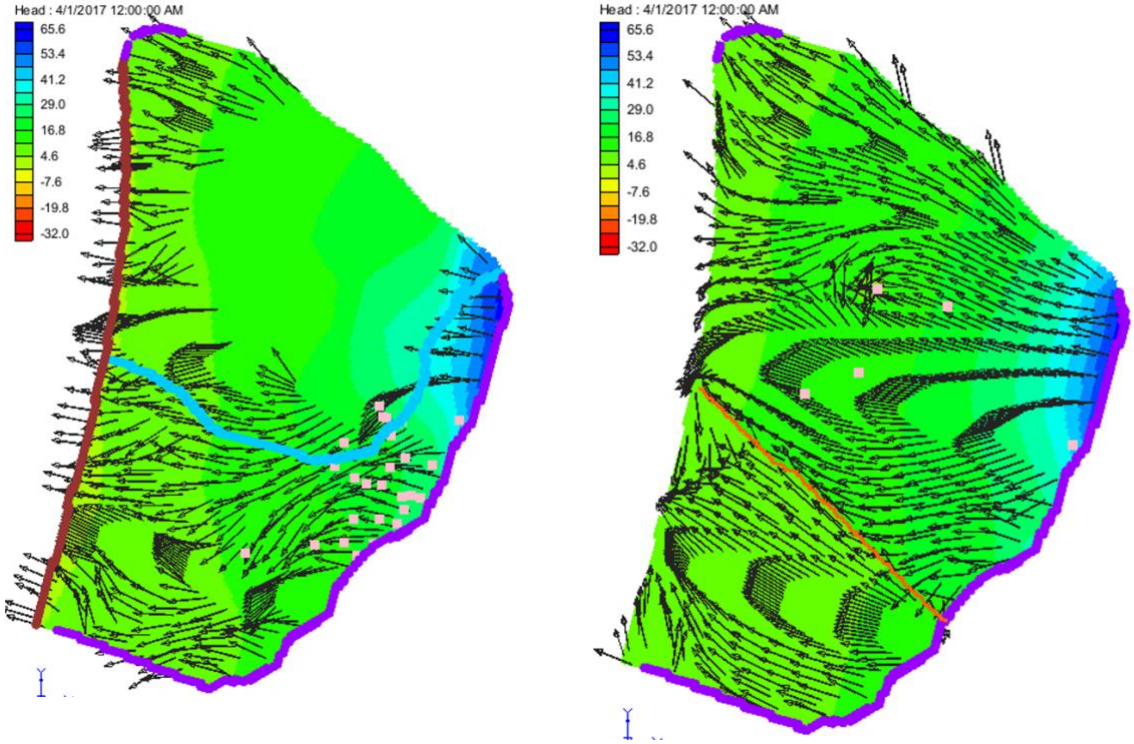

Figure 34. Head and Flow Vectors for Layer 1 (Left) and Layer 3 (Right) on 4/1/2017 (Wells as Pink Squares)

Also, interesting to note is the massive influence and drawdown observed by the Grover Beach Well 4 in the third layer (Figure 31, Right). This well seems to exert a large influence over the entire northern portion's groundwater movement. This is a significant finding, if valid, and could help Grover Beach understand this well's impact on the overall groundwater movement in this formation.

4.2. Flow Budget

The flow budget was examined for general trends over the whole model domain and is shown in Table 10. Storage is the water contained within the cells and is initially a function of the starting head. An influx exists from the transient boundary (called constant head since it's the CHD package), the recharge and stream leakage to the cells. However, the flow from cells out to the stream is almost two orders of magnitude greater than what the cells received, indicating that overall, the stream is recharged by the aquifer in this area. In contrast, the transient boundary shows a net influx to the model with the in magnitude being much larger than the out. The Head Dep. Boundary represents the general head boundary for the ocean and only shows flow out of the cells, which indicates that seawater intrusion is unlikely.

Table 10. Model Flow Budget from January 2008 to December 2019 in Acre-ft

Component	In	Out
Storage	7,663	7,776
CHD	125,857	44,597
Wells	0	39,495
Head Dep. Bound	0	42,183
Recharge	388	0
Stream Leakage	175	8,421
Total	**134,083**	**142,471**

5. Conclusion and Recommendations

5.1. Conclusion

Overall, this study shows success in a highly parameterized calibration for the model with improved model duration, more detailed and discretized recharge estimation, and incorporation of addition municipal well data.

This model was developed using the GMS conceptual model approach with some data pre-processed in ArcMap. Coverages were mapped to a transient MODFLOW-NWT solver using the UPW package with monthly stress periods from January 2008 to December 2019. Once running forward the model was calibrated using a mixed zonal and pilot point PEST approach to minimize error by optimizing parameters.

The optimized parameters were then compared to values and ranges found in previous studies. Most optimized values concurred with these previous studies with the exception of vertical anisotropy. Model statistics such as the correlation coefficient, R-squared, and regression plots were presented and evaluated. At this time the model is a less than ideal fit for the system and should only be used to evaluate overall trends.

The model shows general outflow to the ocean, westerly groundwater movement following wet periods, southernly groundwater movement following dry periods, and significant influence and drawdown from Grover Beach Well 4 in the Careaga Formation.

5.2. Future Recommendations

5.2.1. Modeling

The fundamental component of the model is the grid. While the three layer model was able to represent the NCMA, there are physical features that could be modeled better by improving the grid. The clay layer present in cross section L-L' (Figure 6) from the Santa Maria Groundwater Basin Characterization is approximately 30 to 60 feet thick and most likely causes some significant confinement. The other clay layer, estimated at 10 to 30 feet thick, overlays the contact between the Paso Robles and Careaga Formations (Fugro Consultants, Inc., 2015). The confining layers of clay present within the Paso Robles model could be represented as their own layer due to their probable low hydraulic conductivity. The other grid correction that would most likely improve the model would be the inclusion of the Santa Maria River fault in lieu of a horizontal flow barrier. The barrier is mapped to both the second and third layer when the offset probably only slows, not inhibits, a fraction of this area.

In addition to better modeling of the physical location and offset of the fault, the conductance could also be parameterized. This model set the constant conductance of the horizontal flow barrier representing the fault to zero, which is likely inaccurate. The fault only slows flow, not inhibits, by being a sudden transition between two formations.

Lastly the potential "bullseye" effect from the pilot points in the hydraulic conductivity in layer 2 and the vertical anisotropy in layer 1 and 2 could be improved. The PEST manual suggests changing the distribution of the points and adding further pilot points, which increases the parameters, and allows for more estimation flexibility.

The increase in parameters would most likely dramatically increase the computing time and computing power required for calibration.

5.2.2. Data Collection

While the Santa Maria River fault does have some data suggesting a flow barrier, i.e., the observed 40 ft head difference in the past (GEOSCIENCE & Water Systems Consulting, 2018), no such data exists for the close by Oceano fault. Installing or identifying monitoring wells on either side of the fault and collecting head observations from the multiple formations would be helpful in determining if an impediment exists.

Another point of uncertainty in the model was with the northern boundary along Pismo Creek. While some of this missing information was mitigated by using finished contours from the annual NCMA reports, actual water level data would be more representative and allow for more accurate modeling and confidence in this section of the model.

Lastly, the monitoring well information was usually only available twice to four times a year. These data gaps, between observation data, had straight lines interpolated by MODFLOW at each month (stress period) which may not be completely descriptive of the area. Observations to match the stress period, monthly, would allow for a more complete representation of the area, and give PEST more accurate observations, to refine the model to. The County of San Luis Obispo collects and maintains monitoring well data which most likely has more frequent observations available than in comparison with what was available to this study.

5.2.3. Future Applications

With improvements, this model could be adapted to study areas of potential saltwater intrusion and groundwater depletion under current conditions with greater accuracy. The interaction between the stream and the model could be examined further to determine the precise timing and amount of exchange between the two. Further the model could also be used to simulate the effects of different theoretical agriculture and land use practices on the groundwater availability.

References

Allander, K. K., Niswonger, R. G., & Jeton, A. E. (2014). *Simulation of the Lower Walker River Basin Hydrologic System, West-Central Nevada, Using PRMS and MODFLOW Models.* Virginia: USGS.

Berry, L. E., Mutiti, S., & Hazzard, S. (2011). Determining the Hydraulic Conductivity of the Subsurface in Wetland Environments. *American Geophysical Union, H33E-1353*.

Cal Poly Irrigation Training & Reseach Center. (2021, April 15). *California Evapotranspiration Data*. Retrieved May 2021, from ITRC.org: http://www.itrc.org/etdata/index.html

Cleath & Associates. (1996). *Water Resources Management Study for The Woodlands.* San Luis Obispo.

Corvallis Forestry Research Community. (2021, February 10). *Manning's n Values (Chow, 1959)*. Retrieved May 2021, from Geowater: http://www.fsl.orst.edu/geowater/FX3/help/8_Hydraulic_Reference/Mannings_n_Tables.htm

Danapour, M., Højberg, A., Høgh Jensen, K., & Stisen, S. (2019, June 04). Assessment of regional inter-basin groundwater flow using both simple and highly parameterized optimization schemes. *Hydrogeology Journal, 1929-1947*.

Department of Water Resouces. (1979). *Water Resources of the Arroyo Grande Area, Southern District Report.* California Department of Water Resources.

Department of Water Resources. (2002). *Water Resources of the Arroyo Grande- Nipomo Mesa Area.*

Doherty, J. (2004). *PEST, Model-Independent Parameter Estimation.* Watermark Numerical Computing.

Doherty, J. E., & Hunt, R. J. (2010). *Approaches to Highly Parameterized Inversion: A Guide to Using PEST for Groundwater-Model Calibration.* Reston: USGS.

Duffield, G. M. (2019, November 23). *Representative Values of Hydraulic Properties*. Retrieved from AQTESOLV: http://www.aqtesolv.com/aquifer-tests/aquifer_properties.htm#:~:text=An%20anisotropy%20ratio%20relates%20hydraulic,conductivity%20%5BL%2FT%5D.

Fugro Consultants, Inc. (2015). *Northern Cities Management Area 2014 Annual Monitoring Report.* San Luis Obispo: Fugro Consultants, Inc.

Fugro Consultants, Inc. (2015). *Santa Maria Groundwater Basin Characterization and Planning Activities Study.* Atascadero: Fugro Consultants, Inc.

GEOSCIENCE & Water Systems Consulting. (2018). *Central Coast Blue Phase 1B, Technical Memorandum 1: Conceptual Model.* Claremont.

GEOSCIENCE. (2018). *Agricultural Pumping Estimates Technical Memorandum.* Claremont.

GEOSCIENCE. (2018). *Central Coast Blue Phase 1B, Model Boundaries Technical Memorandum.* Claremont.

GEOSCIENCE. (2019). *Central Coast Blue Phase 1B, Technical Memorandum No. 3: Model Calibration.* Claremont: GEOSCIENCE.

Groundwater Foundation. (n.d.). *What is Groundwater?* Retrieved April 2021, from Groundwater.com: https://www.groundwater.org/get-informed/basics/whatis.html

Groundwater Modeling Decision Support Initiative. (n.d.). *Frequently Asked Questions*. Retrieved May 2021, from PEST Home Page: https://pesthomepage.org/frequently-asked-questions

GSI Water Solutions, Inc. (2019). *Northern Cities Management Area 2019 Annual Monitoring Report.* Atascadero.

Harbaugh, A. W. (2005). *MODFLOW-2005, The U.S. Geological Survey Modular Ground-Water Model—the Ground-Water Flow Process.* Retrieved from U.S. Geological Survey Techniques and Methods 6-A16: https://pubs.usgs.gov/tm/2005/tm6A16/PDF.htm

Hunt, R. J., & Feinstein, D. (2012). MODFLOW-NWT: Robust Handling of Dry Cells Using a Newton Formulation of MODFLOW-2005. *Ground Water*, 659-663.

Irmak, S., & Haman, D. Z. (2017, August). *Evapotranspiration: Potential or Reference?* (U. o. Florida, Producer) Retrieved May 2021, from Ask IFAS: https://edis.ifas.ufl.edu/publication/ae256#:~:text=Reference%20evapotranspiration%20(ETo)%3A,0.23%2C%20closely%20resembling%20the%20evapotranspiration

Masterson, J. P., Pope, J. P., Fienen, M. N., Monti, Jr., J., Nardi, M. R., & Finkelstein, J. S. (2016). *Documentation of a Groundwater Flow Model Developed to Assess Groundwater Availability in*

the Northern Atlantic Coastal Plain Aquifer System from Long Island, New York, to North Carolina. Reston: U.S. Geological Survey.

NASA Earth Observatory. (2016). *NASA Earth Observatory*. Retrieved from San Joaquin Valley is Still Sinking: https://earthobservatory.nasa.gov/images/89761/san-joaquin-valley-is-still-sinking

SLO County. (n.d.). *Arroyo Grande Creek Watershed*. Retrieved January 2021, from SLO Watershed Project Snapshots: https://www.slocounty.ca.gov/Departments/Public-Works/Forms-Documents/Projects/SLO-Watershed-Project/SLO-Watershed-Project-Snapshot-South-County-Arroyo.pdf

SLO County. (n.d.). *County of San Luis Obispo*. Retrieved March 2021, from Santa Maria River Valley Groundwater Basin: https://www.slocounty.ca.gov/Departments/Public-Works/Committees-Programs/Sustainable-Groundwater-Management-Act-(SGMA)/Santa-Maria-River-Valley-Groundwater-Basin.aspx

SLO County Department of Agriculture. (2020). *2019 Annual Crop Report.* San Luis Obispo: San Luis Obispo County Department of Agriculture.

Stannard, D. I., Gannett, M. W., Polette, D. J., Cameron, J. M., Waibel, M. S., & Spears, J. M. (2013). Evapotranspiration from Wetland and Open-Water Sites at Upper Klamath Lake, Oregon, 2008–2010. *Scientific Investigations Report 2013–5014*, 44.

State Water Resources Control Board. (2020). *Sustainable Groundwater Management Act Development*. Retrieved May 2021, from Waterboards.ca.gov: https://www.waterboards.ca.gov/water_issues/programs/sgma/development.html

Todd Engineers. (2007). *Water Balance Study for the Northern Cities Area.* Todd Engineers.

USGS. (2004). *A New Streamflow-Routing (SFR1) Package to Simulate Stream-Aquifer Interaction with MODFLOW-2000.* Carson City: U.S. Geological Society.

USGS. (2013). Documentation of the Seawater Intrusion (SWI2) Package for MODFLOW. In USGS, *Book 6, Modeling Techniques* (Vols. Chapter 46 of Section A, Groundwater, p. 22). Reston, Virginia: U.S. Geological Society.

USGS. (2018). *UPW - Upstream Weighting Package*. Retrieved April 2021, from USGS Online Guide to MODFLOW: https://water.usgs.gov/nrp/gwsoftware/modflow2000/MFDOC/index.html?upw_upstream_weighting_package.htm

USGS. (2019, March 4). *MODFLOW-2005: USGS Three-Dimensional Finite-Difference Ground-Water Model*. Retrieved April 2021, from USGS: https://www.usgs.gov/software/modflow-2005-usgs-three-dimensional-finite-difference-ground-water-model

USGS. (2020, March 3). *MODFLOW-NWT: A Newton Formulation for MODFLOW-2005*. Retrieved May 2021, from USGS: https://www.usgs.gov/software/modflow-nwt-a-newton-formulation-modflow-2005

USGS. (n.d.). *California Drought- Comparisons*. Retrieved April 2021, from USGS: https://ca.water.usgs.gov/california-drought/california-drought-comparisons.html

USGS. (n.d.). *California Drought- What is Drought?* Retrieved April 2021, from USGS: https://ca.water.usgs.gov/california-drought/what-is-drought.html#:~:text=During%20times%20of%20drought%2C%20vegetation,intrusion%2C%20and%20damage%20to%20ecosystems.

Wallace, B. M. (2016). *NCMA Groundwater Model, USGS MODFLOW-2005/PEST.*

Worts, G. F. (1951). *Geology and Ground-Water Resources of the Santa Maria Valley Area, California.* Washington D.C.: U.S. Geological Survey.

Zhou, Y., & Li, W. (2011). A review of regional groundwater flow modeling. *GeoScience Fronteirs Volume 2, Issue 2*, 205-214.

Appendix

Reference images from Fugro 2014 Annual NCMA Report (Fugro Consultants, Inc., 2015)

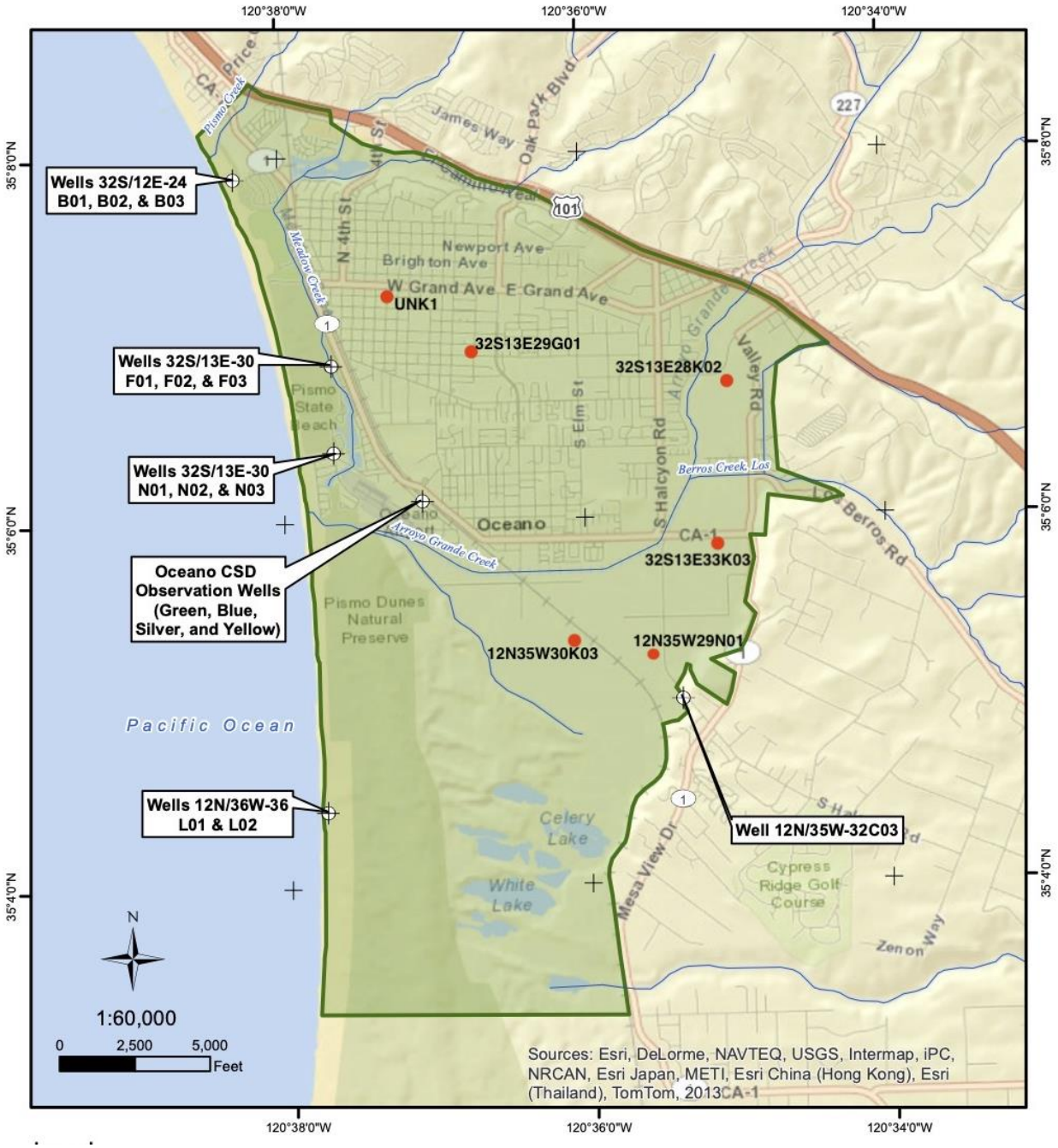

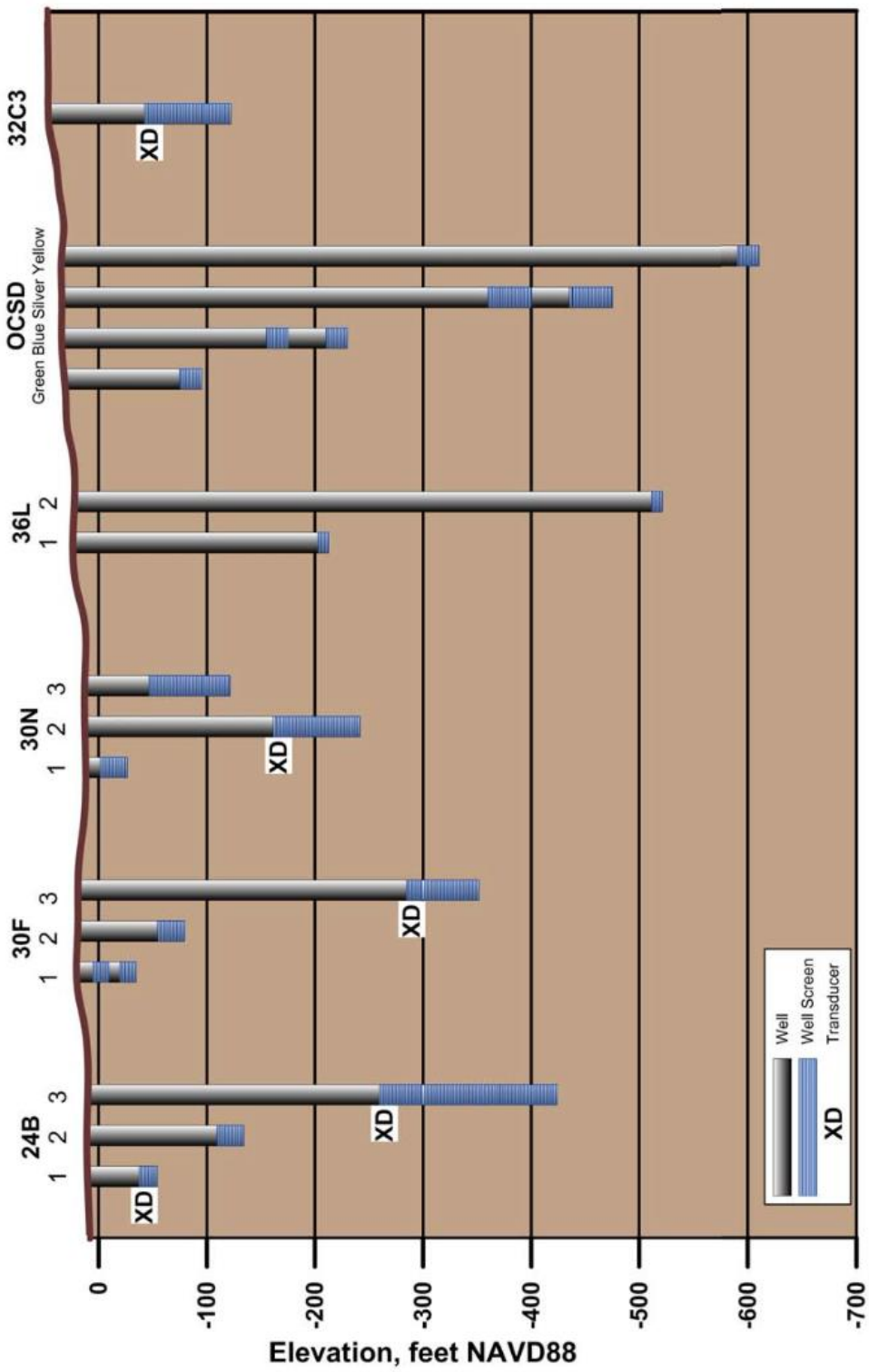
32C3
XD
OCSD
Green Blue Silver Yellow
36L
2
1
30N
3
2
1
XD
30F
3
2
1
XD
24B
3
2
1
XD
XD
Well
Well Screen
Transducer
XD
0
-100
-200
-300
-400
-500
-600
-700
Elevation, feet NAVD88

Sentry Wells (Grouped by Cluster):

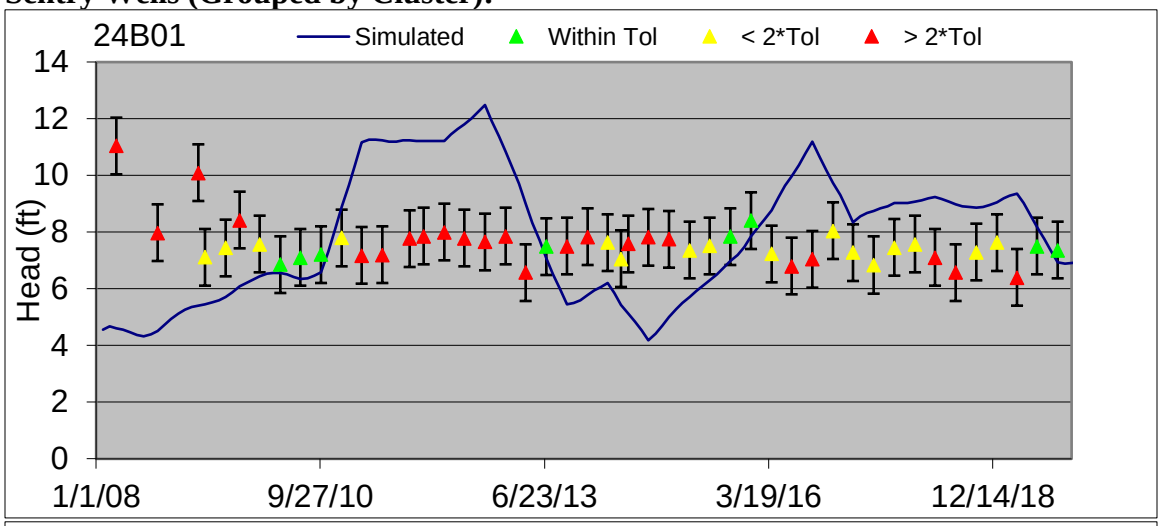

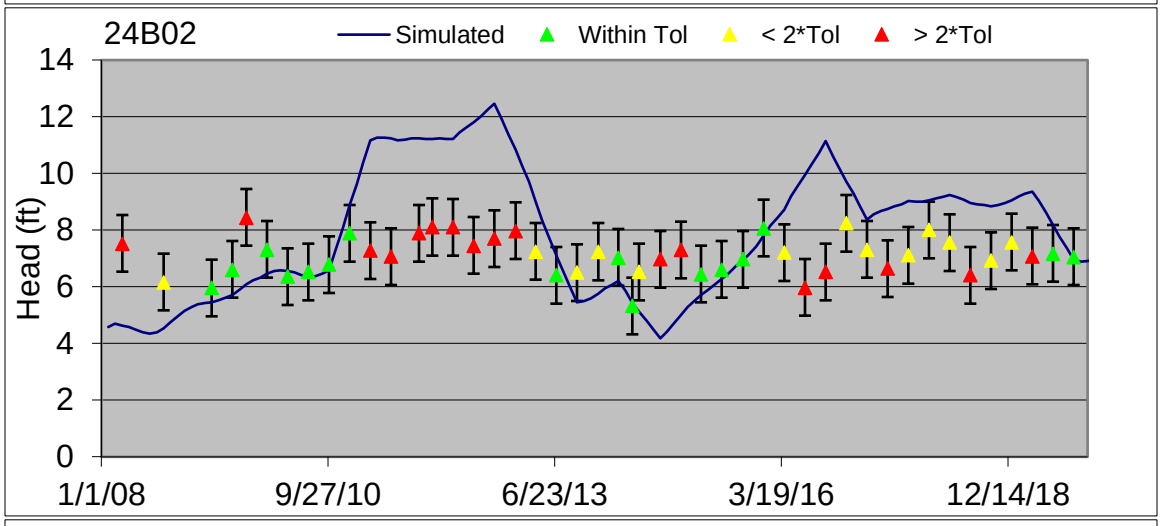

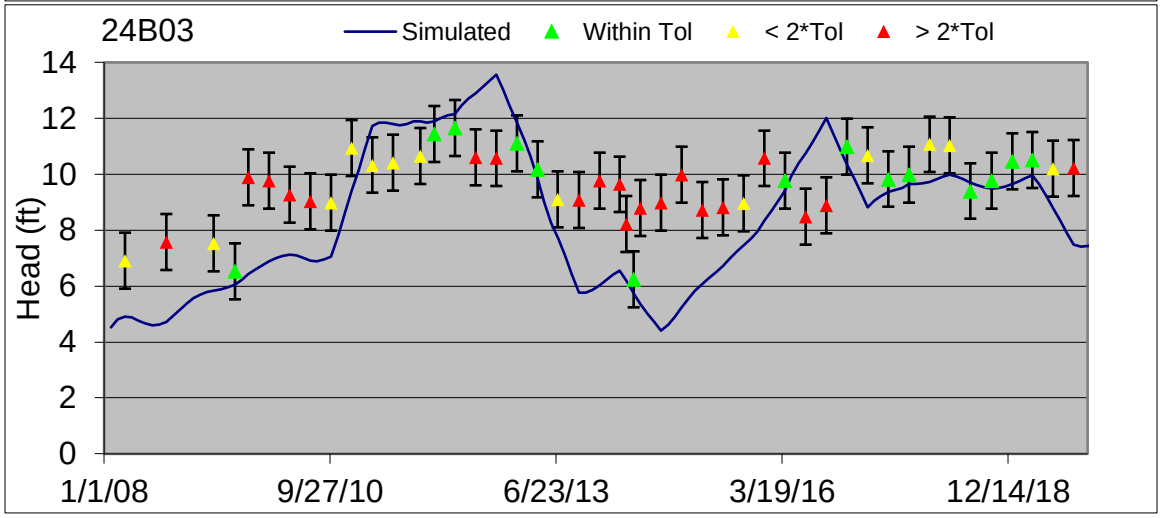

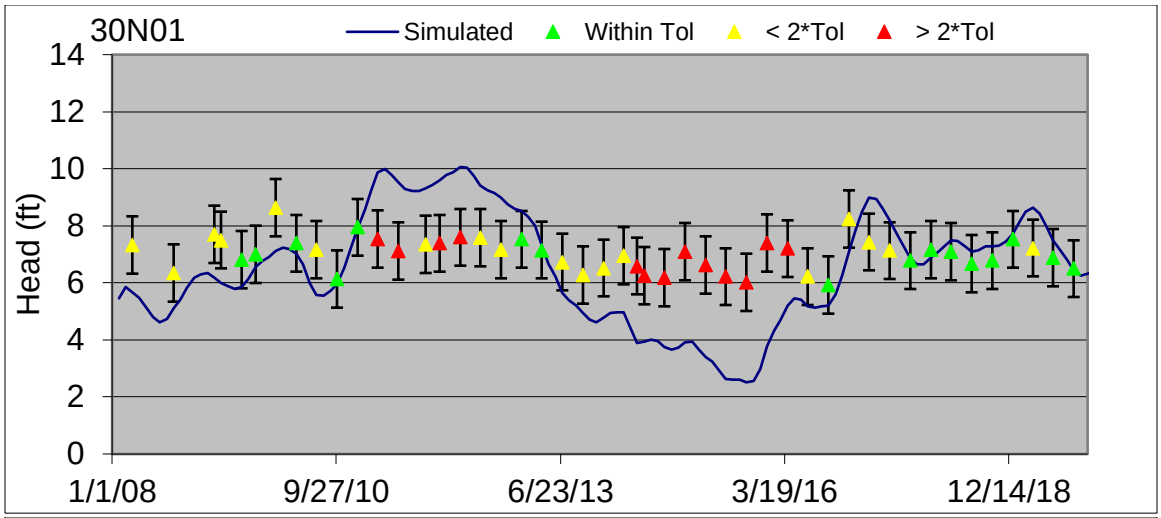
30N01
Simulated
Within Tol
< 2*Tol
> 2*Tol
Head (ft)
14
12
10
8
6
4
2
0
1/1/08
9/27/10
6/23/13
3/19/16
12/14/18

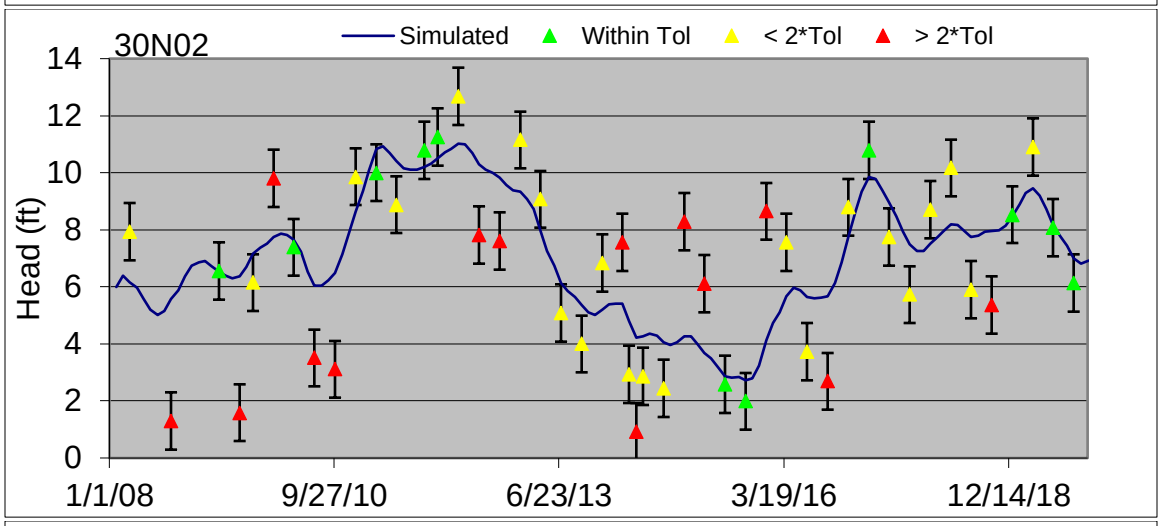
30N02
Simulated
Within Tol
< 2*Tol
> 2*Tol
Head (ft)
14
12
10
8
6
4
2
0
1/1/08
9/27/10
6/23/13
3/19/16
12/14/18

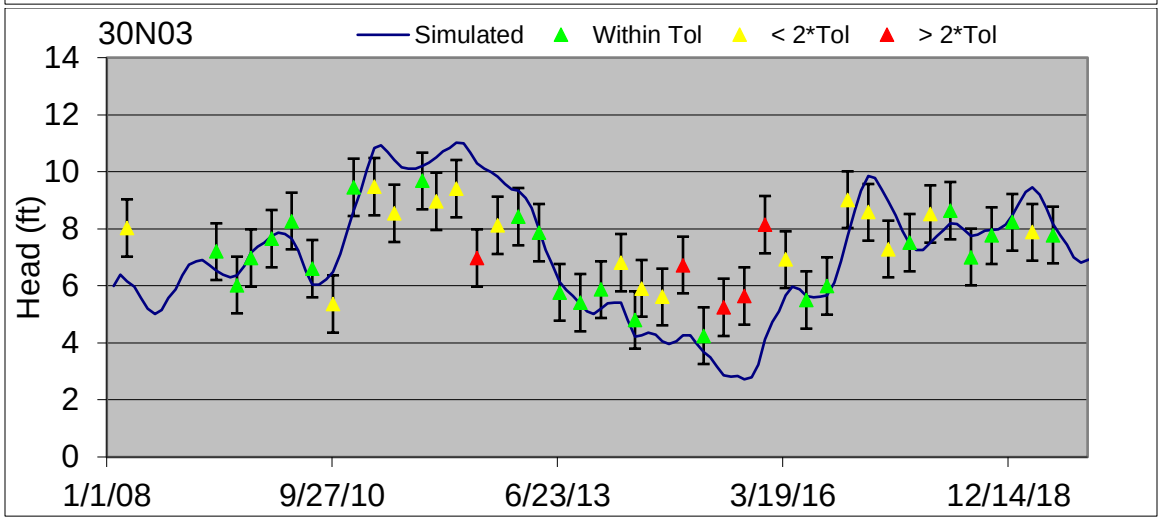
30N03
Simulated
Within Tol
< 2*Tol
> 2*Tol
Head (ft)
14
12
10
8
6
4
2
0
1/1/08
9/27/10
6/23/13
3/19/16
12/14/18

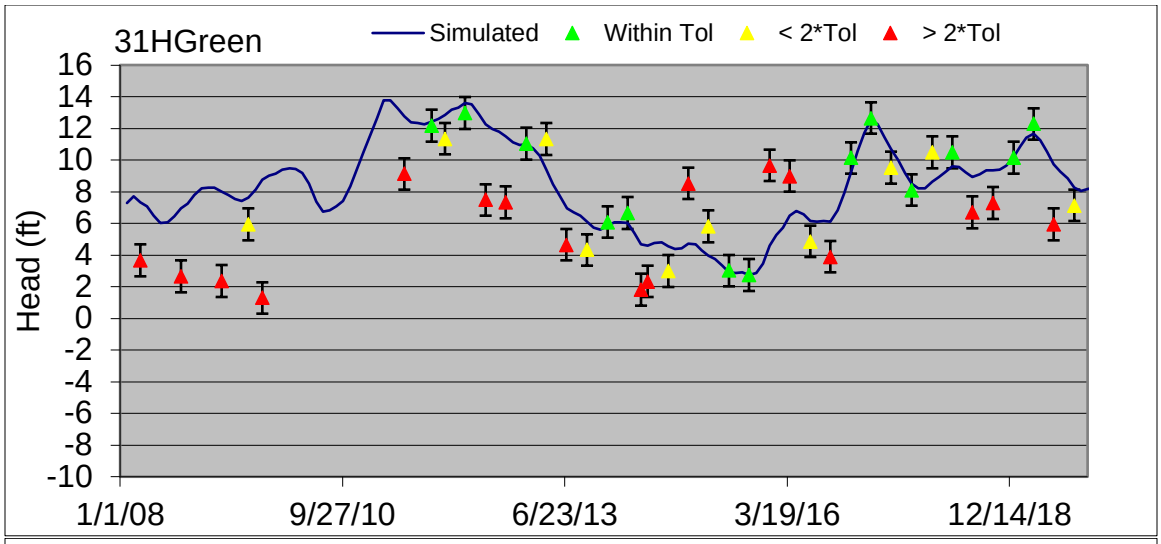
31HGreen
Simulated
Within Tol
< 2*Tol
> 2*Tol
Head (ft)
16
14
12
10
8
6
4
2
0
-2
-4
-6
-8
-10
1/1/08
9/27/10
6/23/13
3/19/16
12/14/18

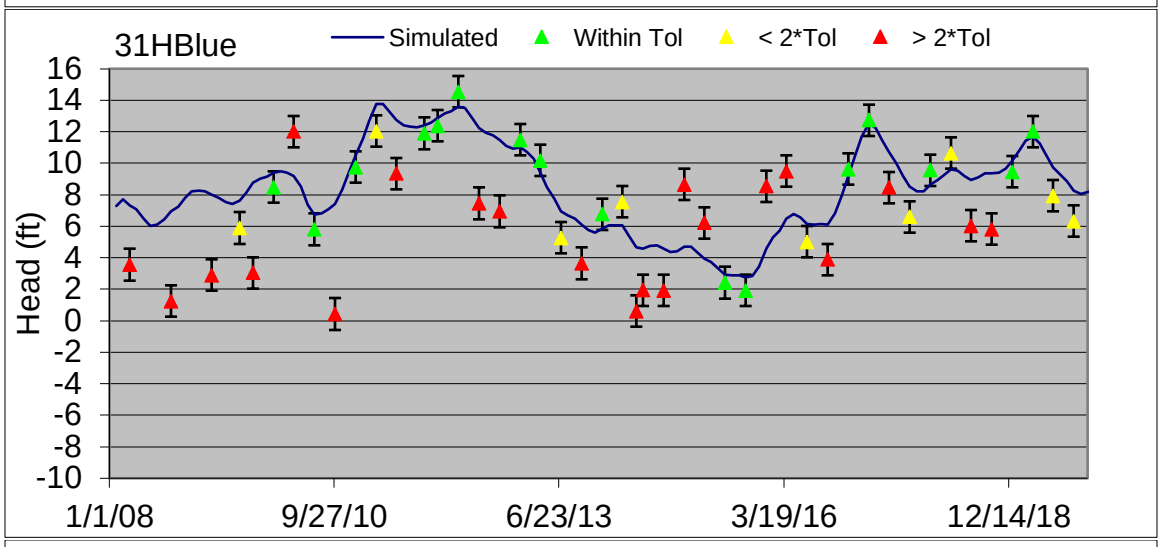
31HBlue
Simulated
Within Tol
< 2*Tol
> 2*Tol
Head (ft)
16
14
12
10
8
6
4
2
0
-2
-4
-6
-8
-10
1/1/08
9/27/10
6/23/13
3/19/16
12/14/18

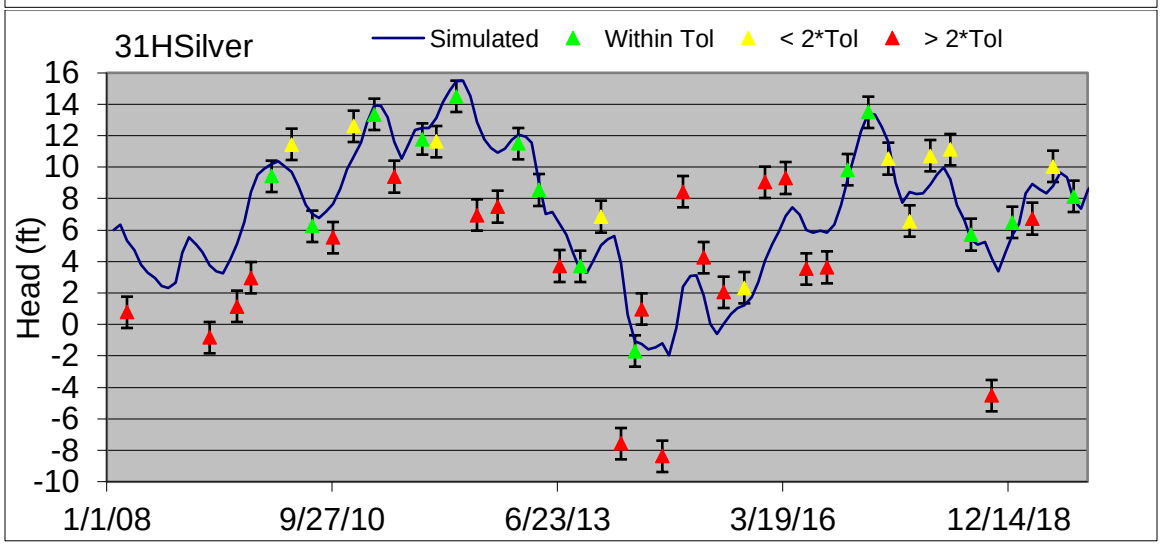
31HSilver
Simulated
Within Tol
< 2*Tol
> 2*Tol
Head (ft)
16
14
12
10
8
6
4
2
0
-2
-4
-6
-8
-10
1/1/08
9/27/10
6/23/13
3/19/16
12/14/18

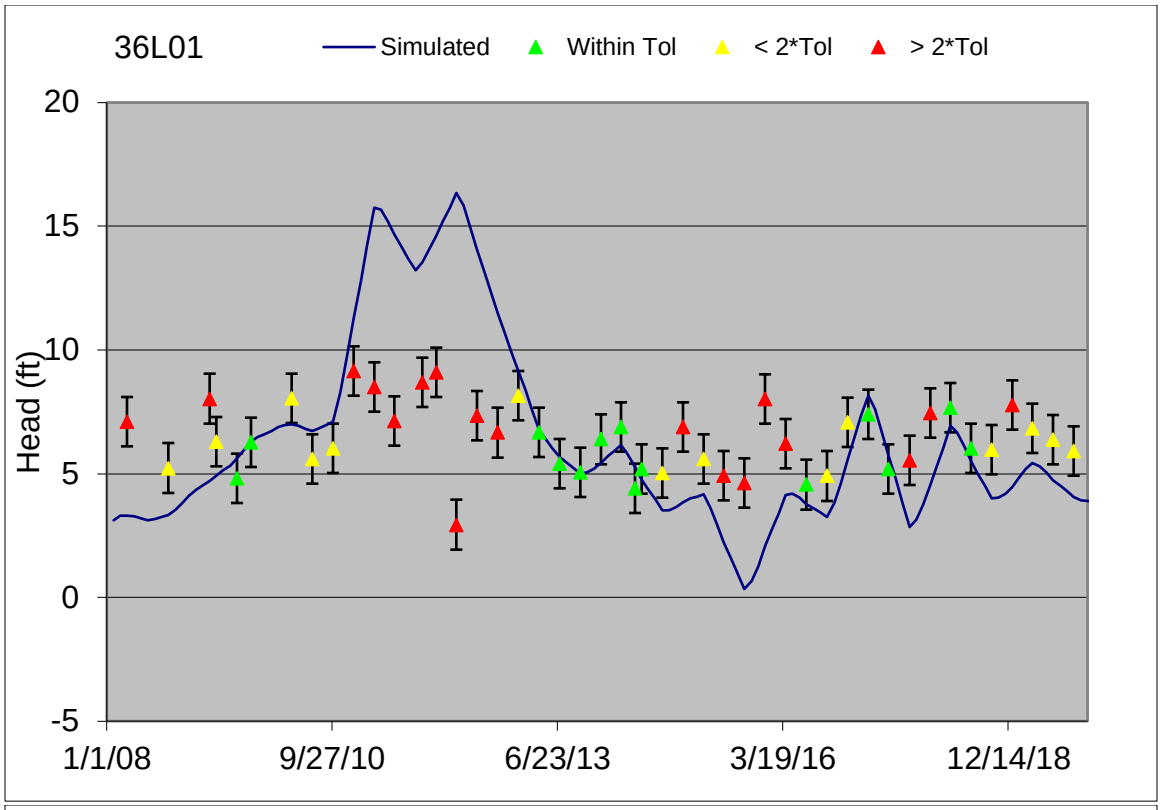
36L01
Simulated
Within Tol
< 2*Tol
> 2*Tol
20
15
10
5
0
-5
Head (ft)
1/1/08
9/27/10
6/23/13
3/19/16
12/14/18

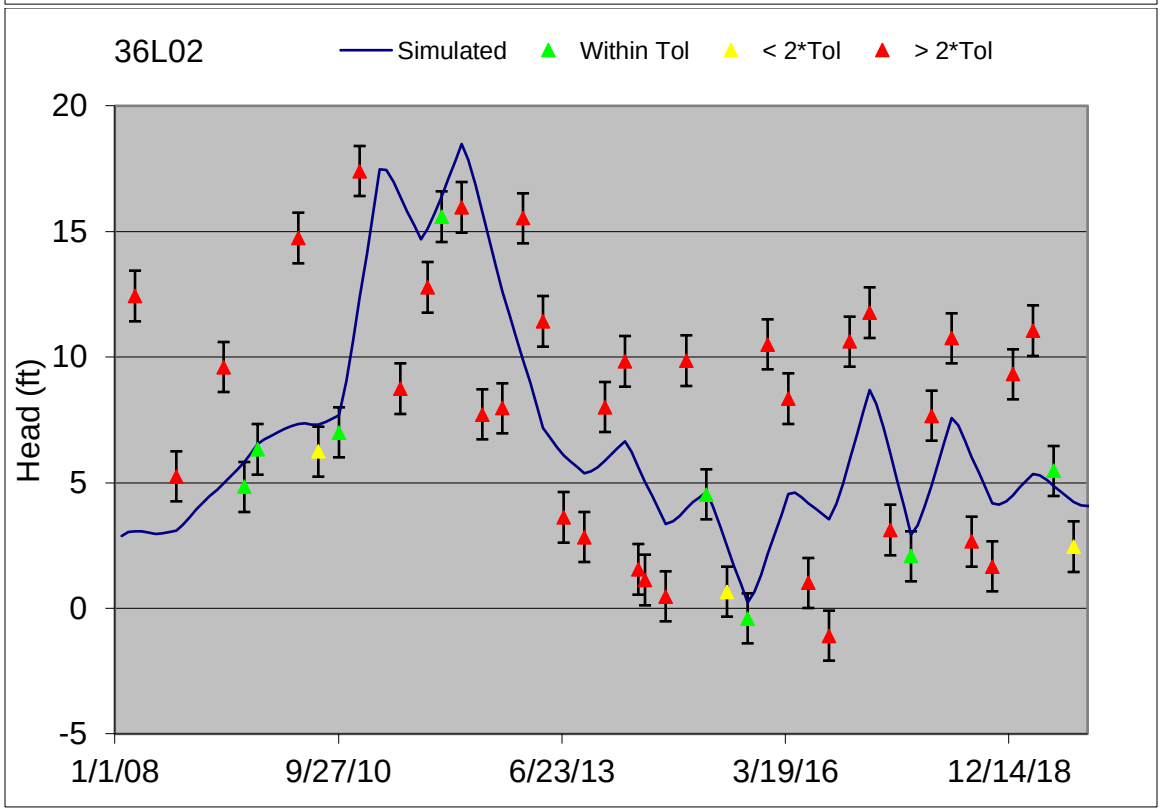
36L02
Simulated
Within Tol
< 2*Tol
> 2*Tol
20
15
10
5
0
-5
Head (ft)
1/1/08
9/27/10
6/23/13
3/19/16
12/14/18

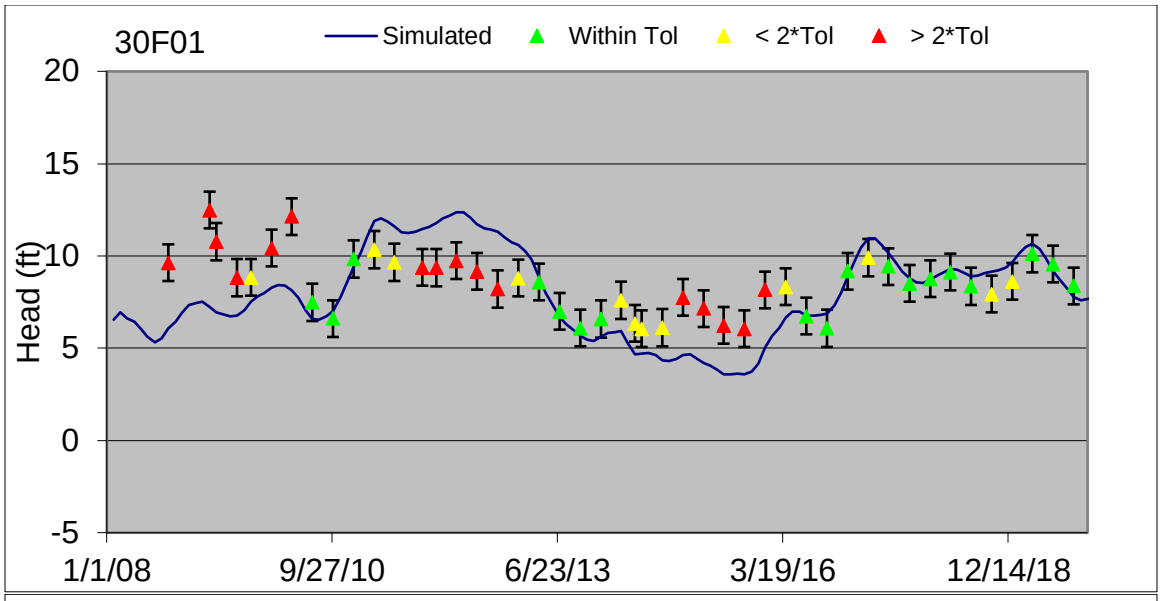
30F01
Simulated
Within Tol
< 2*Tol
> 2*Tol
Head (ft)
20
15
10
5
0
-5
1/1/08
9/27/10
6/23/13
3/19/16
12/14/18

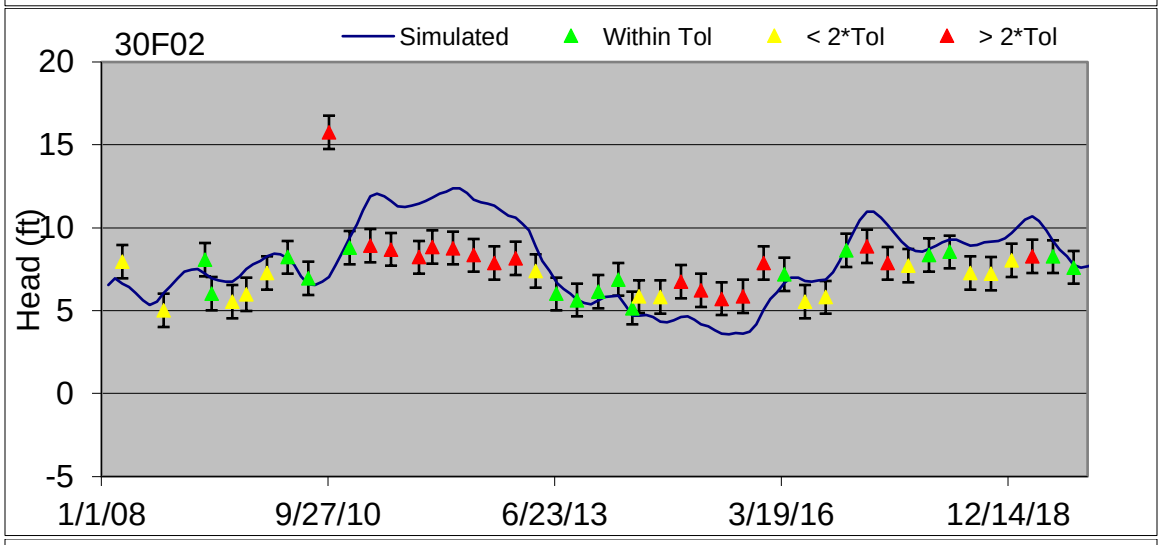
30F02
Simulated
Within Tol
< 2*Tol
> 2*Tol
Head (ft)
20
15
10
5
0
-5
1/1/08
9/27/10
6/23/13
3/19/16
12/14/18

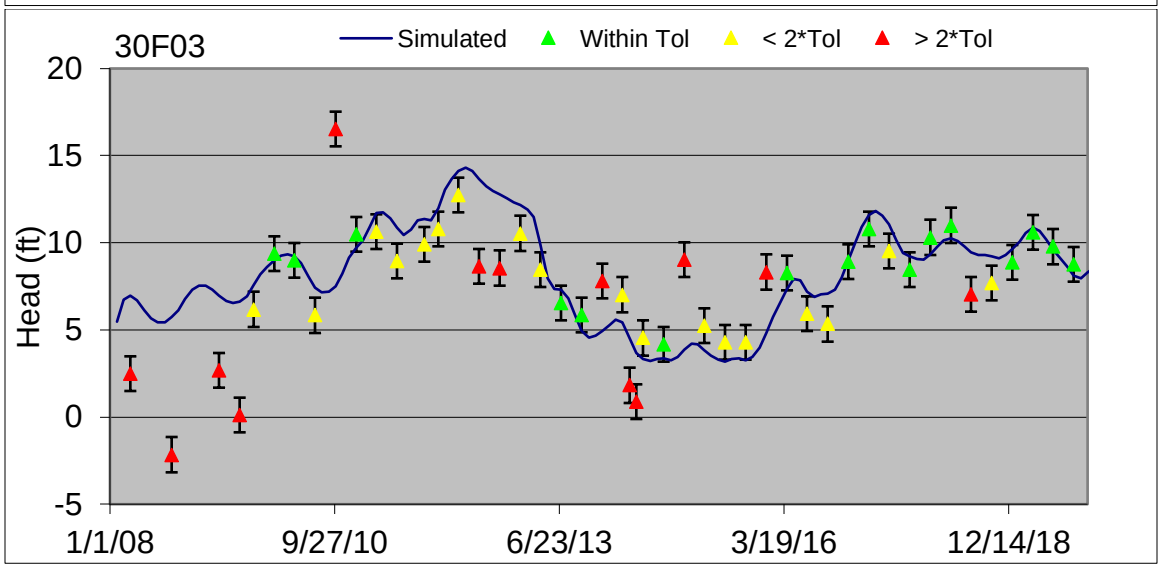
30F03
Simulated
Within Tol
< 2*Tol
> 2*Tol
Head (ft)
20
15
10
5
0
-5
1/1/08
9/27/10
6/23/13
3/19/16
12/14/18

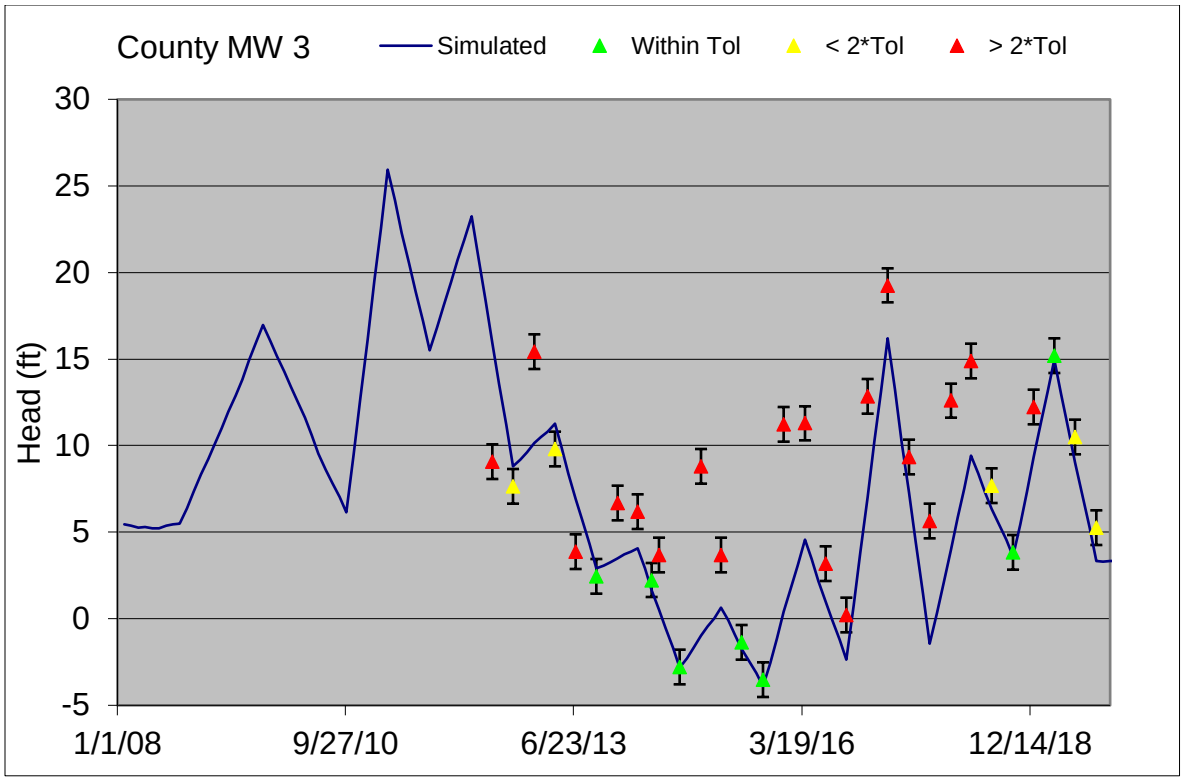
County MW 3
Simulated
Within Tol
< 2*Tol
> 2*Tol
Head (ft)
30
25
20
15
10
5
0
-5
1/1/08
9/27/10
6/23/13
3/19/16
12/14/18

Monitoring Wells:

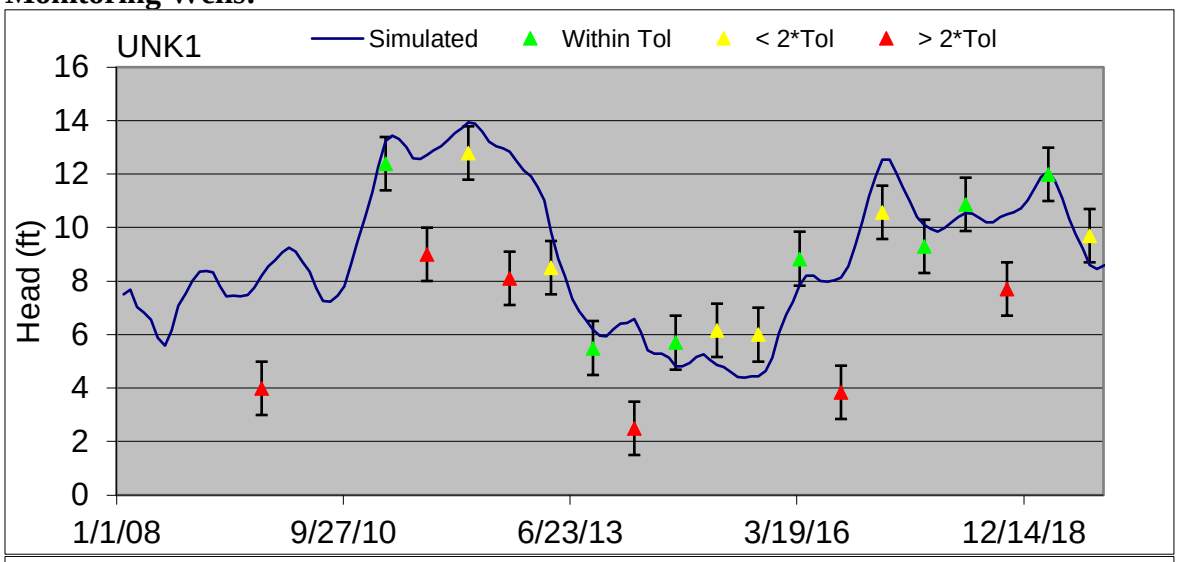

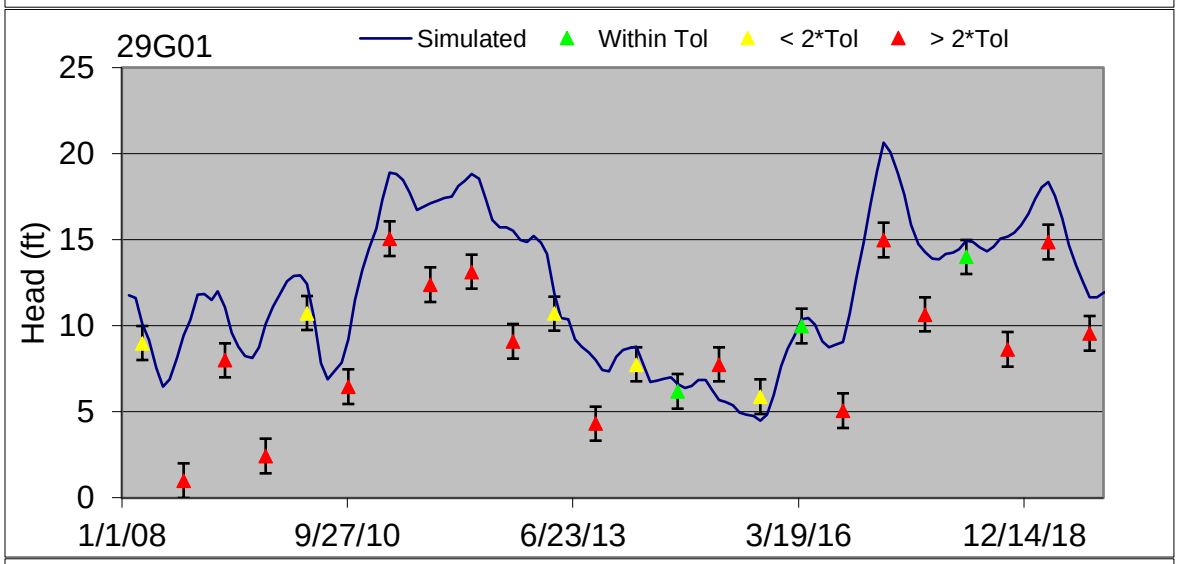

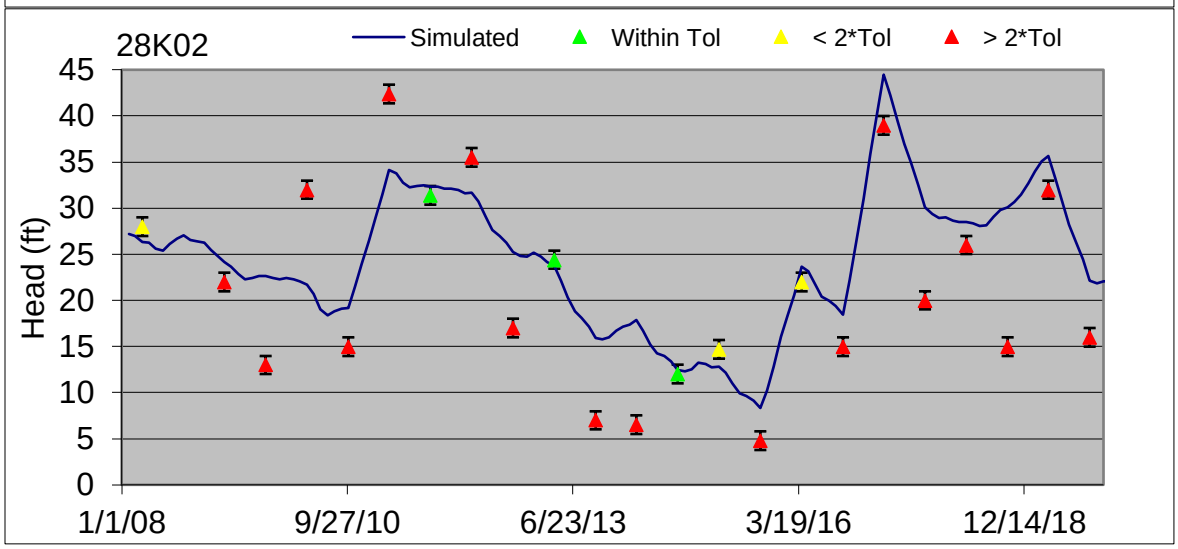

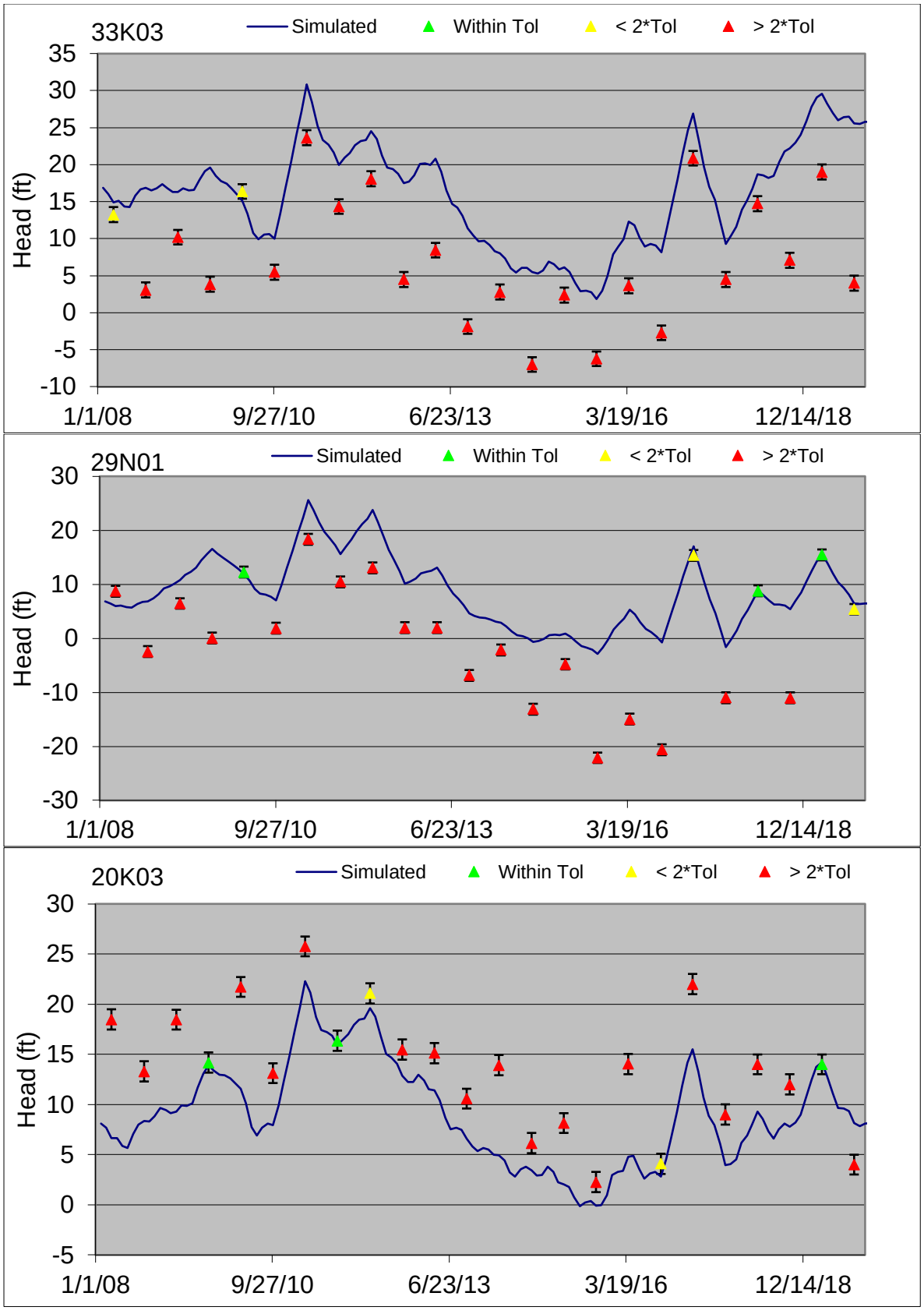
33K03
Simulated
Within Tol
< 2*Tol
> 2*Tol
Head (ft)
35
30
25
20
15
10
5
0
-5
-10
1/1/08
9/27/10
6/23/13
3/19/16
12/14/18
29N01
Simulated
Within Tol
< 2*Tol
> 2*Tol
Head (ft)
30
20
10
0
-10
-20
-30
1/1/08
9/27/10
6/23/13
3/19/16
12/14/18
20K03
Simulated
Within Tol
< 2*Tol
> 2*Tol
Head (ft)
30
25
20
15
10
5
0
-5
1/1/08
9/27/10
6/23/13
3/19/16
12/14/18